NUMERICAL INVESTIGATION OF THE POPULATION DISTRIBUTION IN HETEROGENOUS DOMAIN

A Thesis

by

STEPHEN HENRY

BS, Texas A&M University - Corpus Christi, 2019

Submitted in Partial Fulfillment of the Requirements for the Degree of

MASTER OF SCIENCE

in

MATHEMATICS

Texas A&M University-Corpus Christi
Corpus Christi, Texas

August 2023

NUMERICAL INVESTIGATION OF THE POPULATION DISTRIBUTION IN HETEROGENOUS DOMAIN

A Thesis

by

STEPHEN HENRY

This thesis meets the standards for scope and quality of
Texas A&M University-Corpus Christi and is hereby approved.

Alexey Sadovski, PhD
Chair

Maria Vasilyeva, PhD
Co-Chair

Diane Denny, PhD
Committee Member

M. Muddamallappa, PhD
Committee Member

August 2023

ABSTRACT

We consider the spatial-temporal model of multi-species population distribution in two-dimensional heterogeneous domains. A coupled system of time-dependent diffusion-reaction equations describes the mathematical model of such problems. To solve the problem numerically, we construct an unstructured grid that resolves inclusions on the grid level and produces a semi-discrete system using a finite element method. For time approximation, we apply an explicit-implicit scheme where the reaction term of the equation is taken from the previous time layer. We present numerical results for several test problems to investigate the influence of the geometry and parameters on time to reach equilibrium and the final equilibrium state. An extension of the model is also considered, where we add a memory effect by introducing a time-fractional multi-species model. We derive an implicit finite difference approximation for time discretization based on Caputo's time fractional derivative. A numerical investigation is performed for various orders of the time derivative.

TABLE OF CONTENTS

LIST OF FIGURES

CHAPTER 1: INTRODUCTION

Reaction-diffusion equations are widely used to describe phenomena related to pattern-formation in various biological, chemical, and physical systems [11, 5, 13, 14]. The reaction term naturally appears in various chemistry models to reflect the change in the concentration of one or more chemical species [3, 9, 2, 4]. Chemical reactions transform one substance into another, and the diffusion process causes substances to spread across the spatial domain. Application to the marsh ecosystems for the wetlands at the Nueces River mouth is presented in [12]. In [15], the set of the nonlinear equations is considered for a theory of heat and mass transfer in reactive media and mathematical biology.

In this work, we consider one and two-species models described by unsteady diffusion-reaction equations [22, 21]. The problems in a two-dimensional heterogeneous domain are investigated numerically. We consider a test domain that contains 40 random circle inclusions with varying radii. To construct an accurate approximation by space, we generate unstructured grids that resolve the boundary of the inclusions on the grid level [20, 16, 6]. The discrete system is constructed using the finite element method and semi-implicit time approximation. In semi-implicit time approximation, we approximate the reaction term using the solution from the previous time layer. [18, 8, 17, 19]. Applying such schemes to multispecies interaction models leads to the uncoupled equations for each species which is computationally effective and leads to fast simulations compared with the fully coupled, fully implicit schemes. We present numerical results for three geometries with different volumes of inclusions. The influence of the parameters (diffusion coefficient, expansion rate, and interaction term) is investigated for the one and two-species models. For the one-species model, we present results for two types of heterogeneity and compare results with the case of homogeneous parameters. The time to reach equilibrium is investigated for the different values of the diffusion, expansion rate, and initial conditions. For the two-species model, we present numerical results and consider the influence of the parameters on the final equilibrium state and the time to reach it. Numerical results show a strong impact of heterogeneity on the solution.

The thesis is organized as follows. The first chapter describes the mathematical model for one and two-species populations in the heterogeneous domain. Next, we present the construction of the discrete system based on the finite element method and semi-implicit time approximation in the third chapter. Numerical results and investigation of the influence of the parameters on the solution and final equilibrium state are presented in the fourth chapter. The use of time-fractional diffusion-reaction equations as effective tools for analysing population dynamics in heterogeneous environments is explored in the fifth chapter. Finally, we present the conclusion in the last chapter.

CHAPTER 2: MATHEMATICAL MODEL

This chapter delves into details about building and analysis of mathematical models for population distribution in heterogeneous settings. It specifically focuses on one-species and two-species population models. These models account for population dynamics in regions with various rates of diffusion and expansion. The boundary conditions, initial conditions, and diffusion-reaction equations provide the foundation of the mathematical framework. These problems are approximated spatially using the finite element method, while their temporal derivative is approximated temporally using the finite difference method. Our objective is to have a full understanding of population distribution in heterogeneous environments Ω that can be used to investigate and solve real ecological issues. This thesis introduces the mathematical models for one-species and two-species population distribution in heterogeneous areas. The heterogeneity in various domains is demonstrated by varied expansion rates and diffusion coefficients, which results in the development of diffusion-reaction equations together with an initial condition and boundary conditions.

The numerical solution of these problems using the finite element method to approximate the spatial component and the finite difference approximation for the temporal derivative is a major part of this section. By using this method, a variational issue and its corresponding linear and bilinear forms are derived. In this work, we consider the followig two models

- One-species population model.
- Two-species population model.

The spatial-temporal models of population distribution are considered in heterogeneous domains Ω. Let Ω be the two- dimensional heterogeneous domain

$$\Omega = \Omega_1 \cup \Omega_2,$$

where Ω_1 is the main domain, and Ω_2 is the subdomain related to the inclusions (see Figure 2.1). The formulation of a numerical solution method for these initial-boundary value problems is a key aspect of this part. We use the Finite Element Method for spatial approximation and a finite difference approach for temporal approximation in an effort to deliver an accurate yet computa-

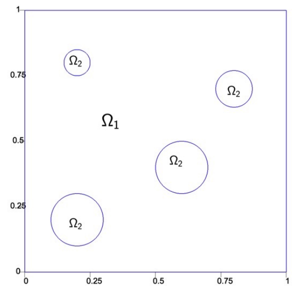

Figure 2.1: Illustration of the heterogeneous domain, $\Omega = \Omega_1 \cup \Omega_2$.

tionally practical solution. With this combination, we are able to create a discrete counterpart of the continuous issue that preserves all of its essential characteristics and enables for numerical computation.

2.0.1 One-Species Population Model

The mathematical model is described by the following diffusion-reaction equation for $u(x,t)$

$$\frac{\partial u}{\partial t} - \nabla \cdot (k(x)\nabla u) = r(x)(1-u)u, \quad x \in \Omega, \quad 0 < t < T, \tag{2.1}$$

where $u(x,t)$ is the population of the species at time t, r is the expansion rate and k is the diffusion coefficient.

We consider equation (2.1) in heterogeneous domains and set

$$k(x) = \begin{cases} k_1, & x \in \Omega_1, \\ k_2, & x \in \Omega_2, \end{cases} \quad r(x) = \begin{cases} r_1, & x \in \Omega_1, \\ r_2, & x \in \Omega_2, \end{cases}$$

We supplement the model with the following initial condition

$$u(x,t=0) = u_0, \quad x \in \Omega, \tag{2.2}$$

and the boundary conditions

$$-k\frac{\partial u}{\partial n} = 0, \quad x \in \partial\Omega, \quad 0 < t < T, \tag{2.3}$$

where n is the outer normal vector to boundary $\partial\Omega$.

For numerical solution of the initial - boundary value problem (2.1) - (2.3), we use a Finite Element Method for approximation by space. To approximate given parabolic equation, we use the following finite difference approximation for time derivative

$$\frac{\partial u}{\partial t} \approx \frac{u^{n+1} - u^n}{\tau},$$

where τ is the given time step and $u^n = u(x,t^n)$, $\tau = T/N$, N is the number of time steps, n is the time layer, $n = 1,2,...,N$. For initial condition, we have $u^0 = u_0$.

Let $V = \{v \in H^1(\Omega) : v = 0,\ x \in \Gamma_1\}$. where $H^1(\Omega)$ is the Sobolev space containing functions v such that v^2 and $\left|\nabla v^2\right|$ have finite integrals over Ω. To write a variational formulation of the problem, we multiply the equation (4.15) by the test function v and integrate over the domain Ω. Using integration-by-parts formula

$$-\int_\Omega \nabla \cdot (k(x)\nabla u)\ v\ dx = \int_\Omega k(x)\nabla u \cdot \nabla v\ dx - \int_{\partial\Omega} k(x)\frac{\partial u}{\partial \nu}\ v\ ds$$

where ν is the unit vector to the boundary $\partial\Omega$.

After applying boundary conditions (4.17), we have the following variational formation: find $u \in V$ such that

$$\int_\Omega \frac{u^{n+1} - u^n}{\tau}\ v\ dx - \int_\Omega k(x)\nabla u^{n+1} \cdot \nabla v\ dx = \int_\Omega r(x)u^{n+1}(1-u^n)\ v\ dx, \quad \forall v \in V.$$

We note that, we used a explicit-implicit time approximation.

Next, we rewrite vatiational formulation in the following form: find $u \in V$ such that:

$$a(u^{n+1},v) = L(v), \quad \forall v \in V,$$

where bilinear and linear forms are defined as follows

$$a(u,v) = \frac{1}{\tau}\int_\Omega u\ v\ dx + \int_\Omega k(x)\nabla u \cdot \nabla v\ dx + \int_\Omega r(x)u(1-u^n)\ v\ dx,$$

$$L(v) = \frac{1}{\tau}\int_\Omega u^n\ v\ dx.$$

Let $\mathcal{T}^h$ be a partition of the domain Ω that resolve inclusions on the grid level with mesh size h. Let $V_h \subset V$ contains functions which are piecewise linear in each fine-grid element K. Therefore, we have following discrete variational formulation: find $u_h \in V_h$ such that

$$a(u_h^{n+1},v) = L(v), \quad \forall v \in V,$$

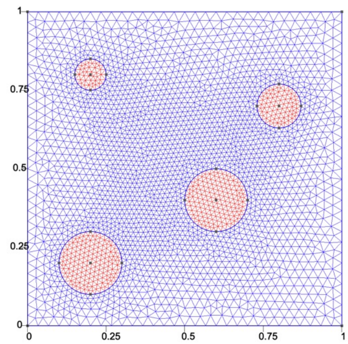

Figure 2.2: Illustration of the computational mesh with triangular cells, $\mathcal{T}^h$.

We can write the above discrete systems in the matrix form as follows

$$A_h U_h^{n+1} = F_h^u, \text{where}, \tag{2.4}$$

$$U_h^{n+1} = [u_j^{n+1}], \quad A_h = [a_{ij} = a(\psi_i, \psi_j)], \quad F_h^u = [f_j = l_u(\psi_j)],$$

with linear basis function $\psi_i \in \mathbb{P}_1$. The size of the discrete system is $DOF = N_h$, where N_h is the number of fine grid nodes. Finally, we have the following algorithm:

- Set initial condition $u_h^n = u_0$ for $n = 0$.
- For $n = 1,2,...,$ we solve system of linear equations (4.18) to find U_h^{n+1} for given solution from previous time step U_h^n.

This section leads us through the methodical, step-by-step construction of the one-species population model. We have worked through the complexities of the initial and boundary conditions starting with the formulation of the diffusion-reaction equation and have come out with a practical mathematical model. This model not only accurately depicts the current scientific issue, but it also paves the road for careful examination. The study of numerical methods, especially the Finite Element Method and finite difference approximations, was then explored after the formulation. Through this investigation, we learned how we can transform our ongoing problem into a discrete one that can be resolved with the helpof pythoncode. The section's conclusion was a discrete variational formulation, a mathematical idea that connects the discrete and continuous domains.

2.0.2 Two-Species Population Model

Next, we consider the two-species competition model. The mathematical model is described by the following system of nonlinear diffusion-reaction equations for $u^{(1)}(x,t)$ and $u^{(2)}(x,t)$

$$\begin{aligned} \frac{\partial u^{(1)}}{\partial t} - \nabla \cdot \left(k_1(x) \nabla u^{(1)}\right) &= r_1(x)(1-u^{(1)})u^{(1)} - \alpha_{12}(x) u^{(1)} u^{(2)}, \quad x \in \Omega, \quad 0 < t < T, \\ \frac{\partial u^{(2)}}{\partial t} - \nabla \cdot \left(k_2(x) \nabla u^{(2)}\right) &= r_2(x)(1-u^{(2)})u^{(2)} - \alpha_{21}(x) u^{(1)} u^{(2)}, \quad x \in \Omega, \quad 0 < t < T, \end{aligned} \tag{2.5}$$

where $u^{(1)}(x,t)$ and $u^{(2)}(x,t)$ are the population of the species at time t, r_1 and r_2 are the expansion rates for the fist and second species, k_1 and k_2 are the diffusion coefficients, and α_{12} and α_{21} are the competition coefficients between species 1 and 2, and 2 and 1.

In heterogeneous domain $\Omega = \Omega_1 \cup \Omega_2$, we set

$$k_\zeta(x) = \begin{cases} k_\zeta^m, & x \in \Omega_1, \\ k_\zeta^c, & x \in \Omega_2, \end{cases} \quad r_\zeta(x) = \begin{cases} r_\zeta^m, & x \in \Omega_1, \\ r_\zeta^c, & x \in \Omega_2, \end{cases}, \quad \zeta = 1,2.$$

and

$$\alpha_{12}(x) = \begin{cases} \alpha_{12}^m, & x \in \Omega_1, \\ \alpha_{12}^c, & x \in \Omega_2, \end{cases}, \quad \alpha_{21}(x) = \begin{cases} \alpha_{21}^m, & x \in \Omega_1, \\ \alpha_{21}^c, & x \in \Omega_2, \end{cases}$$

We consider the system of equations (2.5), with the following initial conditions

$$u^{(1)}(x,t=0) = u_{01}, \quad u^{(2)}(x,t=0) = u_{02}, \quad x \in \Omega, \tag{2.6}$$

and boundary conditions

$$-k_1 \frac{\partial u^{(1)}}{\partial n} = 0, \quad -k_2 \frac{\partial u^{(2)}}{\partial n} = 0, \quad x \in \partial\Omega, \quad 0 < t < T. \tag{2.7}$$

For both one-species population models and two-species population models, we have made great progress in this section towards the numerical solution of initial-boundary value problems. We developed finite difference approximations for the problem's time derivative using a semi-implicit time approximation. By employing a solution from the prior temporal layer to evaluate the reaction portion of the problems, this strategy also allowed us to linearize the problem and produce a set of forms for the one- and two-species models.

The foundation for comprehending population distribution in varied locations has been established by this chapter. With initial and boundary conditions, the mathematical models for populations of one and two species are now complete. We have been able to convert continuous problems into discrete concerns that are manageable in terms of processing by using the finite element and finite difference methods. Through further study and simulations using these techniques, we can learn a lot about ecological dynamics and population behaviour. The numerical results and discussions from the computational approach used to create the models are presented in the next sections, which will throw light on the complex interactions and phenomena displayed by various populations in varied environments. Next, we present an approximation of the model using the finite element method for approximation by space and semi-implicit time approximation.

CHAPTER 3: APPROXIMATION BY SPACE AND TIME

For both one-species and two-species population models, the numerical solution of the initial-boundary value problems is the main topic of this chapter. Applying semi-implicit approximation by time as the initial step in this attempt entails using finite difference approximation to handle the time derivative. By using this strategy, we are able to linearize the problems and generate particular forms for each model. The variational formulation for both models is then presented, offering a mathematical foundation for resolving challenging population dynamics in heterogeneous settings. The part also emphasises the essential relationship between species, providing a glimpse into the complexity of multi-species relationships. The Finite Element Method for space-based approximation is then introduced, along with the discrete systems. For the numerical solution of the initial - boundary value problems for one and two-species population models, we first apply semi-implicit approximation by time. We use the following finite difference approximation for the time derivative

$$\frac{\partial v}{\partial t} \approx \frac{v^{n+1} - v^n}{\tau},$$

where τ is the given time step and $v^n = v(x,t^n)$, $\tau = T/N$, N is the number of time steps, n is the time layer, $n = 1,2,\ldots,N$. We linearize a problem by evaluating the reaction part using a solution from the previous time layer and obtain the following forms:

- One-species model

$$\frac{u^{n+1} - u^n}{\tau} - \nabla \cdot \left(k(x)\nabla u^{n+1}\right) = r(x)(1-u^n)u^n, \quad x \in \Omega, \quad n = 1,2,\ldots,N \tag{3.8}$$

- Two-species model

$$\begin{aligned} \frac{u^{(1),n+1} - u^{(1),n}}{\tau} - \nabla \cdot \left(k_1(x)\nabla u^{(1),n+1}\right) &= r_1(x)(1-u^{(1),n})u^{(1),n} - \alpha_{12}(x)u^{(1),n}u^{(2),n}, \\ \frac{u^{(2),n+1} - u^{(2),n}}{\tau} - \nabla \cdot \left(k_2(x)\nabla u^{(2),n+1}\right) &= r_2(x)(1-u^{(2),n})u^{(2),n} - \alpha_{21}(x)u^{(1),n}u^{(2),n}, \end{aligned} \tag{3.9}$$

where $x \in \Omega$ and $n = 1,2,\ldots,N$.

Our analysis was supported by the semi-implicit approximation by time and the finite difference approximation for the time derivative. By separating into one-species and two-species models, we have not only provided an in-depth understanding of these systems but have also outlined their intricate connections and functionality within the context of population dynamics. These formulas represent a major advancement in our numerical investigation and set the basis for the following sections.

3.0.1 Variational Formulation

To write a variational formulation of the problem, we multiply the equation by the test function and integrate it over the domain Ω. For the one-species model, we have the following variational formulation: find $u \in V$ such that

$$\int_\Omega \frac{u^{n+1} - u^n}{\tau} \, v \, dx - \int_\Omega k(x) \nabla u^{n+1} \cdot \nabla v \, dx = \int_\Omega r(x) u^n (1 - u^n) \, v \, dx, \quad \forall v \in V, \tag{3.10}$$

where $V = H^1(\Omega)$. We rewrite variational formulation in the following form: find $u \in V$ such that:

$$a(u^{n+1}, v) = L(v), \quad \forall v \in V,$$

where bilinear and linear forms are defined as follows

$$\begin{aligned} a(u,v) &= \frac{1}{\tau} \int_\Omega u \, v \, dx + \int_\Omega k(x) \nabla u \cdot \nabla v \, dx, \\ L(v) &= \frac{1}{\tau} \int_\Omega u^n \, v \, dx - \int_\Omega r(x) u^n (1 - u^n) \, v \, dx. \end{aligned}$$

For the two-species model, we have the following variational formulation

$$\begin{aligned} &\int_\Omega \frac{u^{(1),n+1} - u^{(1),n}}{\tau} \, v^1 \, dx - \int_\Omega k_1(x) \nabla u^{(1),n+1} \cdot \nabla v^1 \, dx \\ &\qquad = \int_\Omega r_1(x) u^{(1),n} (1 - u^{(1),n}) \, v^1 \, dx - \int_\Omega \alpha_{12}(x) u^{(1),n} u^{(2),n} \, v^1 \, dx, \\ &\int_\Omega \frac{u^{(2),n+1} - u^{(2),n}}{\tau} \, v^2 \, dx - \int_\Omega k_2(x) \nabla u^{(2),n+1} \cdot \nabla v^2 \, dx \\ &\qquad = \int_\Omega r_2(x) u^{(2),n} (1 - u^{(2),n}) \, v^2 \, dx - \int_\Omega \alpha_{21}(x) u^{(1),n} u^{(2),n} \, v^2 \, dx, \end{aligned} \tag{3.11}$$

for $\forall v^1 \in V^1$ and $v^2 \in V^2$ with $V^1 = V^2 = H^1(\Omega)$. We rewrite variational formulation in the following form: find $u^{(1)} \in V^1$ and $u^{(2)} \in V^2$ such that

$$\begin{aligned} a^1(u^{(1),n+1}, v^1) &= L^1(v^1), \quad \forall v^1 \in V^1, \\ a^2(u^{(2),n+1}, v^2) &= L^2(v^2), \quad \forall v^2 \in V^2, \end{aligned} \tag{3.12}$$

where bilinear and linear forms are defined as follows

$$a^{\zeta}(u^{(\zeta)},v^{\zeta}) = \frac{1}{\tau}\int_{\Omega} u^{(\zeta)}\ v^{\zeta}\ dx + \int_{\Omega} k_{\zeta}(x)\nabla u^{(\zeta)}\cdot\nabla v^{\zeta}\ dx, \quad \zeta = 1,2,$$

$$L^{\zeta}(v^{\zeta}) = \frac{1}{\tau}\int_{\Omega} u^{(\zeta)}\ v^{\zeta}\ dx + \int_{\Omega} r_{\zeta}(x)u^{(\zeta),n}(1-u^{(\zeta),n})\ v^{i}\ dx - \int_{\Omega} \alpha_{\eta,\zeta}(x)u^{(\eta),n}u^{(\zeta),n}\ v^{\zeta}\ dx,$$

for $\eta,\zeta = 1,2$ and $\eta \neq \zeta$. We note that the systems are decoupled and can be solved separately for each species. The variational formulations of the one-species and two-species population models are presented in this section, which effectively provides a starting point for the development of intuitive approaches and methods for the resolution of these models. The elaborations comprise weak form transformations that are appropriate, test space forms that are appropriate, and the formation of relevant bilinear and linear forms. Additionally, by determining the proper bilinear and linear forms for each species, the section clarifies the mechanics of multi-species interactions within a shared domain and emphasises the complexity of the two-species model.

3.0.2 Discrete System

Let $\mathcal{T}^h$ be a triangulation of the domain Ω

$$\mathcal{T}^h = \cup_{i=1}^{N_h^c} K_i,$$

where N_h^c is the number of cells. We suppose that triangulation is resolving inclusions on the grid level with mesh size h. Next, we define discrete spaces on grid $\mathcal{T}^h$. Let $V_h \subset V$ contains functions which are piecewise linear in each fine-grid element K_i. Therefore, we have the following discrete variational formulations

- One-species model: Find $u_h \in V_h$ such that

$$a(u_h^{n+1},v_h) = L(v_h), \quad \forall v_h \in V_h,$$

and we have the following matrix form

$$A_h U_h^{n+1} = F_h, \tag{3.13}$$

where

$$U_h^{n+1} = [u_j^{n+1}], \quad A_h = [a_{ij} = a(\psi_i,\psi_j)], \quad F_h = [f_j = l(\psi_j)].$$

- Two-species model: Find $u_h^{(1),n+1} \in V_h$ and $u_h^{(2),n+1} \in V_h$ such that

$$a_1(u_h^{(1),n+1}, v_h^1) = L_1(v_h^1), \quad \forall v_h^1 \in V_h,$$
$$a_2(u_h^{(2),n+1}, v_h^2) = L_2(v_h^2), \quad \forall v_h^2 \in V_h,$$

and we have the following matrix form for each species

$$A_h^\zeta U_h^{(\zeta),n+1} = F_h^\zeta, \quad \zeta = 1,2, \tag{3.14}$$

where

$$U_h^{(\zeta),n+1} = [u_j^{(\zeta),n+1}], \quad A_h^\zeta = [a_{i,ij}^\zeta = a^\zeta(\psi_i, \psi_j)], \quad F_h^\zeta = [f_j^\zeta = l^\zeta(\psi_j)].$$

Here we use a linear basis function $\psi_i \in \mathbb{P}_1$. Therefore, the size of the discrete system for each species is $DOF = N_h^v$, where N_h^v is the number of fine grid nodes. The discretization of the continuous variational formulations of the one-species and two-species population models using a piecewise linear basis inside an appropriate grid domain has been thoroughly described in this section. The solution procedure is then made simpler by converting the formulas to a matrix form. The strength of this method comes in its inherent adaptability and computing efficiency, which are essentially determined by the number of fine grid nodes that specify the degrees of freedom of the system. This renders it an essential step in the process because these features lay the way for solving intricate biological population models. The discrete system's size further emphasises the need to strike a compromise between accuracy goals and available computing power. Future study will think about utilising more sophisticated computational approaches to effectively solve these discrete systems.

To sum up, this chapter is an essential first step in comprehending and solving the one-species and two-species population models. We started by linearizing the problems by utilising a semi-implicit time approximation and finite difference to approximate the time derivative. In order to describe the dynamics of species populations in varied habitats, we were able to define the variational problems as a result. The discrete systems are provided as matrices and serve as the building blocks for effective and useful numerical solutions. These ideas and computational tools make it possible to investigate complex ecological phenomena that would otherwise be difficult to analyse analytically. This chapter provides the required tools to increase our understanding of complicated population dynamics and their implications for ecological studies by integrating approximation approaches, variational formulations, and the Finite Element Method.

CHAPTER 4: NUMERICAL RESULTS

The behaviour of a mathematical model depicting the dynamics of biological species in the domain $\Omega = [0,1]^2$ is examined in this chapter. The model is based on a set of partial differential equations that account for the species rates of diffusion and expansion. Three test geometries are taken into consideration, each of which has 40 circles with different radii but set positions to evaluate the performance of the model. These test geometries, referred to as Geometry 1, 2, and 3, have different main domain and inclusion volume fractions. The visualisation is accomplished using the Paraview programme, while the numerical simulations are carried out using a finite element method. We solve problem in domain $\Omega = [0,1]^2$ and consider three test geometries with small, medium, and large inclusions. The chapter's objectives are to analyse the length of time needed for the system to attain equilibrium in each scenario and look into the impact of various parameters on the dynamics of the final fix. In each geometry, we have 40 circles with the same position and varying radius. Geometries and computational grids (Figure 4.3)

- Geometry 1 with $|\Omega_1| = 0.56$ and $|\Omega_2| = 0.44$. Grid with 92,844 cells and 46,783 nodes.
- Geometry 2 with $|\Omega_1| = 0.8$ and $|\Omega_2| = 0.2$. Grid with 91,352 cells and 46,037 nodes.
- Geometry 3 with $|\Omega_1| = 0.9$ and $|\Omega_2| = 0.1$. Grid with 89,460 cells and 45,091 nodes.

Here $|\Omega_1|$ and $|\Omega_2|$ are the main domain's volume and the inclusions' volume. We simulate with $\tau = 1$ and set initial conditions $u_0 = 0.5$ (one species model) and $u_{01} = u_{02} = 0.5$ (two species model). Geometries with corresponding grids are constructed using Gmsh [7]. Numerical imple-

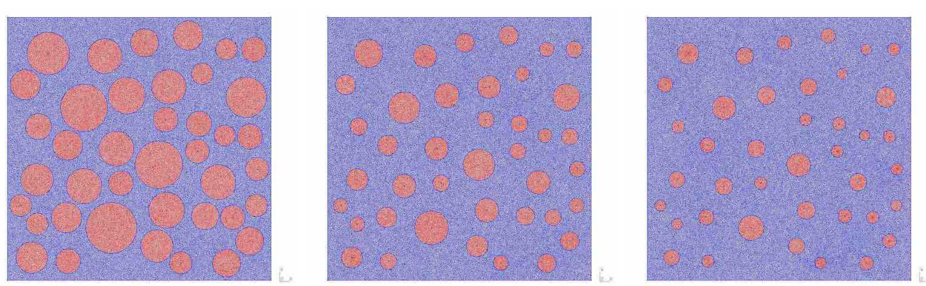

(a) Geometry 1 (b) Geometry 2 (c) Geometry 3

Figure 4.3: Computational grids for Geometry 1, 2 and 3 (from left to right)

mentation is based on the open-source finite element library FEniCS [10]. The Paraview program is used for visualization [1]. In three test geometries with different inclusions, the study examines the dynamics of biological organisms. Gmsh is used to build computational grids, and FEniCS is used to carry out numerical simulations. The findings show how heterogeneity and homogeneity affect the time it takes for one-species and two-species models to reach equilibrium. The endpoint equilibrium state is substantially influenced by diffusion and expansion rates. The biological systems in varied habitats are better understood as a result of this study, which also has implications for managing ecosystems and conserving biodiversity.

4.0.1 One-Species Model

First, we consider the one-species model. We calculate the average value of the solution in subdomain Ω_1 and Ω_2

$$u_m(t) = \frac{1}{|\Omega_1|}\int_{\Omega_1} u(x,t)\ dx, \quad u_c(t) = \frac{1}{|\Omega_2|}\int_{\Omega_2} u(x,t)\ dx,$$

where $|\Omega_i|$ is the volume of domain Ω_i. To calculate the time to reach the equilibrium state, we find a difference between the current solution and the solution from the previous time step

$$|\bar{u}_i^{n+1} - \bar{u}_i^n| < \epsilon, \quad \forall i = 1,2,$$

with $\epsilon = 10^{-5}$. We perform simulations for 1000 time layers. We consider three cases of the parameters:

- Heterogeneity 1, where inclusions have a lower diffusion and lower expansion rate:

$$k(x) = \begin{cases} \tilde{k}, & x \in \Omega_1, \\ \tilde{k}/100, & x \in \Omega_2, \end{cases} \qquad r(x) = \begin{cases} \tilde{r}, & x \in \Omega_1, \\ \tilde{r}/10, & x \in \Omega_2, \end{cases}$$

- Heterogeneity 2, where main domain have a lower diffusion and lower expansion rate:

$$k(x) = \begin{cases} \tilde{k}/100, & x \in \Omega_1, \\ \tilde{k}, & x \in \Omega_2, \end{cases} \qquad r(x) = \begin{cases} \tilde{r}/10, & x \in \Omega_1, \\ \tilde{r}, & x \in \Omega_2, \end{cases}$$

- Homogeneous case, where we set the same coefficients in the main domain and inclusions:

$$k = \tilde{k}, \quad r = \tilde{r}, \quad x \in \Omega.$$

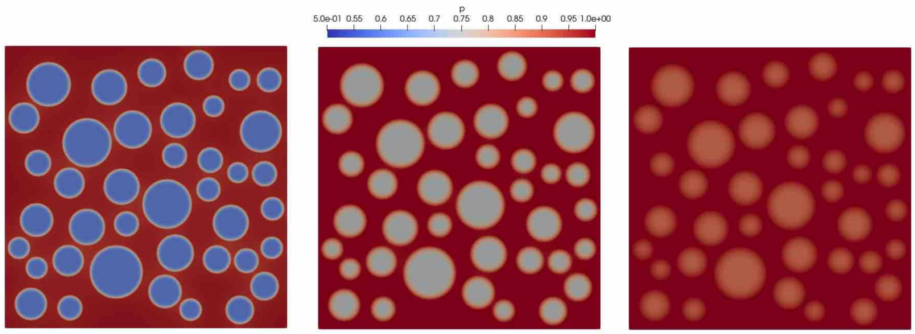

(a) Geometry 1

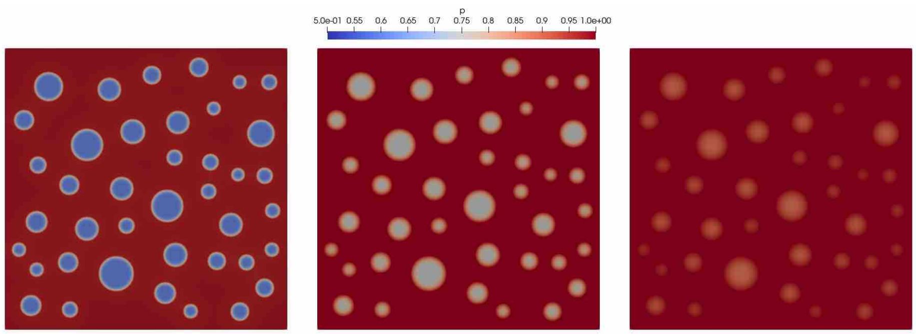

(b) Geometry 2

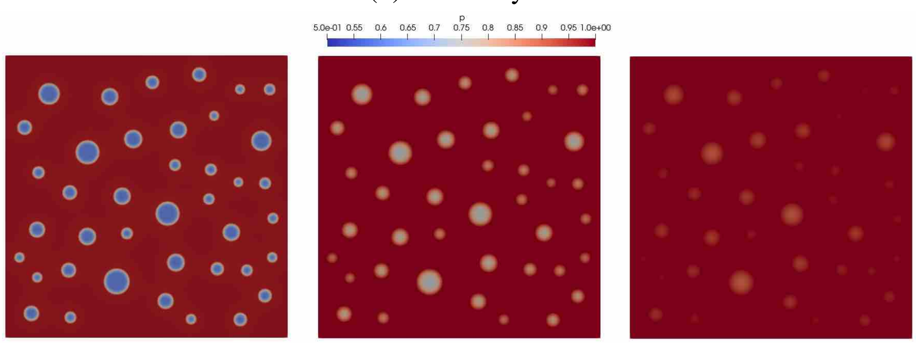

(c) Geometry 3

Figure 4.4: One-species model. Heterogeneity 1. Dynamic of the solution at three time layers $t = 40, 100$, and 200 (from left to right)

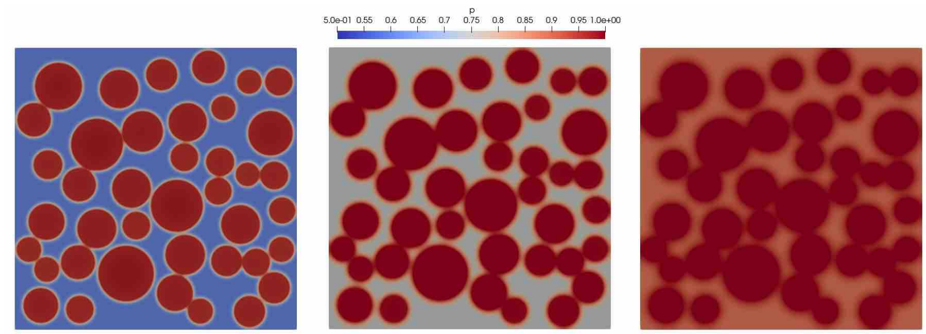

(a) Geometry 1

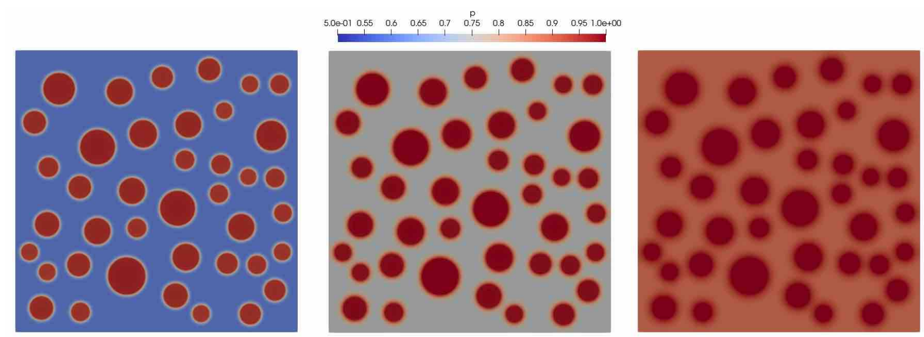

(b) Geometry 2

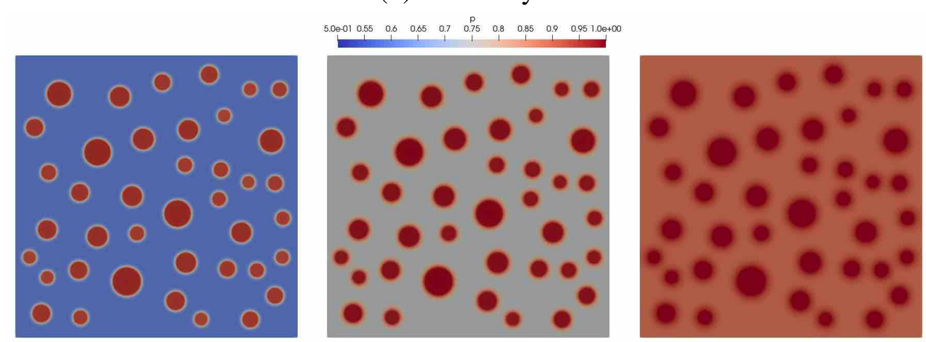

(c) Geometry 3

Figure 4.5: One-species model. Heterogeneity 2. Dynamic of the solution at three time layers $t = 40, 100$, and 200 (from left to right)

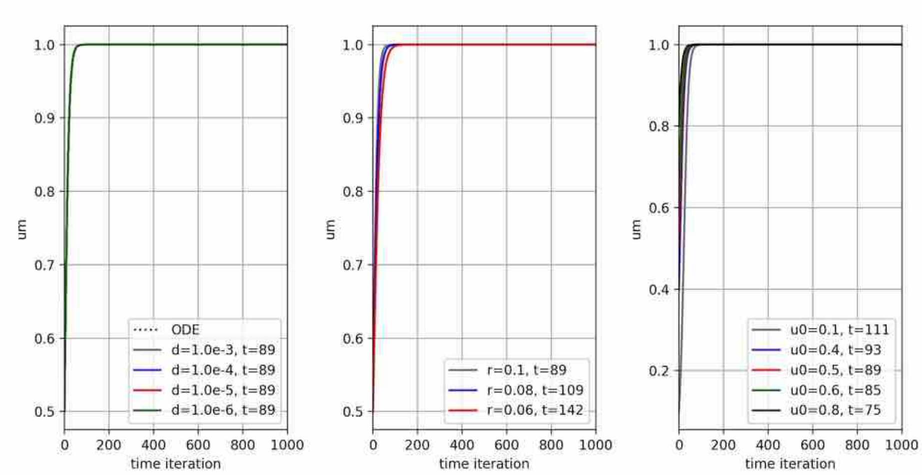

Figure 4.6: One-species model. Homogeneous case. Effect of diffusion, expansion rate, and initial condition (from left to right)

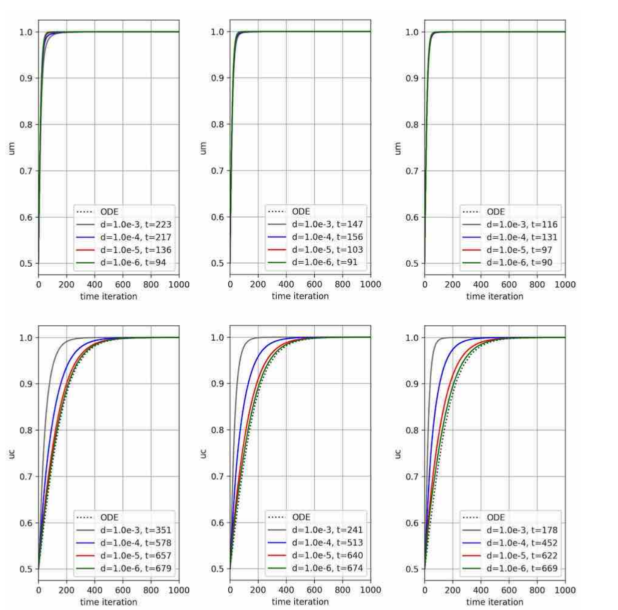

(a) Heterogeneity 1. Geometry 1, 2 and 3 (from left to right).

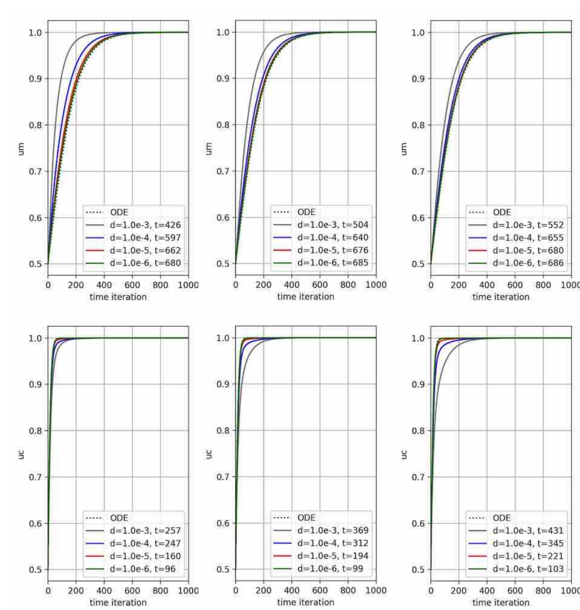

(b) Heterogeneity 2. Geometry 1, 2 and 3 (from left to right).

Figure 4.7: One-species model. Effect of diffusion. First row: $u_m \in \Omega_1$. Second row: $u_c \in \Omega_2$

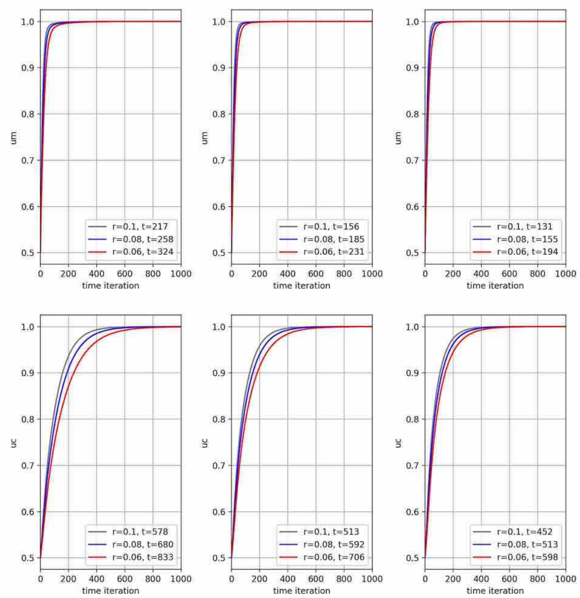

(a) Heterogeneity 1. Geometry 1, 2 and 3 (from left to right).

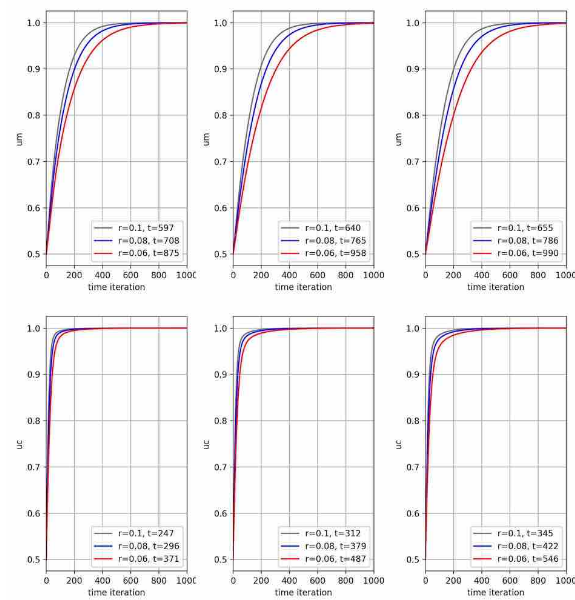

(b) Heterogeneity 2. Geometry 1, 2 and 3 (from left to right).

Figure 4.8: One-species model. Effect of expansion rate. First row: $u_m \in \Omega_1$. Second row: $u_c \in \Omega_2$

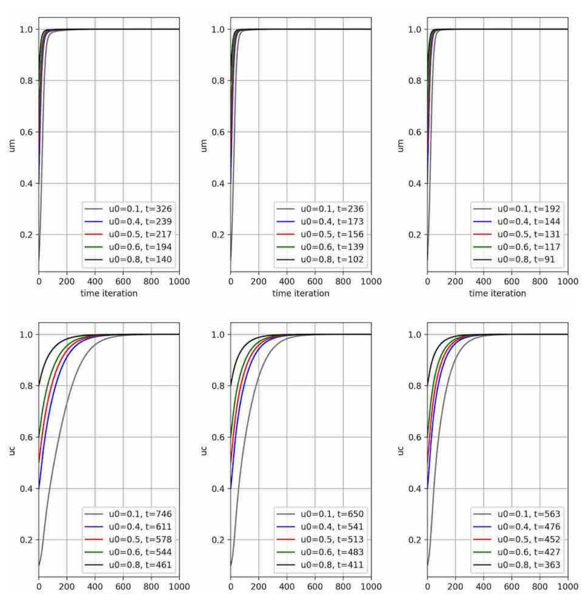

(a) Heterogeneity 1. Geometry 1, 2 and 3 (from left to right).

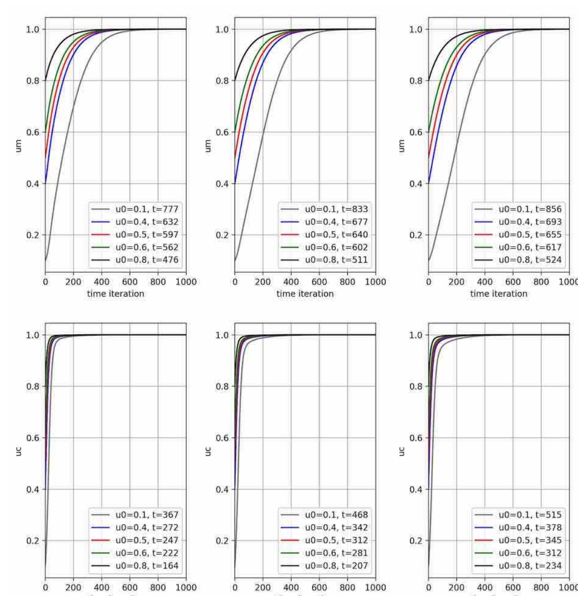

(b) Heterogeneity 2. Geometry 1, 2 and 3 (from left to right).

Figure 4.9: One-species model. Effect of initial condition. First row: $u_m \in \Omega_1$. Second row: $u_c \in \Omega_2$

A homogeneous case is used only for comparison with two types of heterogeneity.

In Figures 4.4 and 4.5, we present solution at three time layers $t = 40, 100$, and 200 to illustrate the dynamic of the solution for two cases of the heterogeneity on three geometries. Results are presented for $\tilde{k} = 10^{-4}$ and $\tilde{r} = 0.1$. We observe the effect of the inclusion radius on the solution dynamic, which is similar for both types of heterogeneity. We see that the time to reach equilibrium is different for three geometries and related to the fraction of the domain filled with inclusions.

In Figure 4.6, we present the dynamic of the solution for the Homogeneous case. In the first picture, the results are presented for different diffusion values $\tilde{k} = 10^{-3}, 10^{-4}, 01^{-5}, 10^{-6}$ and 0 (ordinary differential equations, ODE) are presented with $\tilde{r} = 0.1$ and $u_0 = 0.5$. We observe the same behavior with the same time to reach equilibrium for the homogeneous case. The second picture in Figure 4.6 represent influence of the expansion rate ($\tilde{r} = 0.1, 0.08$ and 0.06) for $\tilde{k} = 10^{-4}$ and $u_0 = 0.5$. We observe the larger time to reach equilibrium for smaller expansion rate with $t = 109$ for $\tilde{r} = 0.08$ and $t = 142$ for $\tilde{r} = 0.06$. The third picture represents the influence of the initial conditions, where we see that time is larger when the distance from the initial condition to final state is larger. For example, we have $t = 111$ for $u_0 = 0.1$ and $t = 75$ for $u_0 = 0.8$.

The time to reach equilibrium for different diffusion coefficients $\tilde{k} = 10^{-3}, 10^{-4}, 01^{-5}$ and 10^{-6} is presented in Figure 4.7 for heterogeneous case. The expansion rate and initial condition are fixed $\tilde{r} = 0.1$ and $u_0 = 0.5$. The solution of the ODE is also depicted in each figure to highlight the effect of the diffusion into the solution. It is well-known that the one-species model converges to the solution $u = 1$ in Ω for the case with free boundary conditions. For Geometry 1, 2 and 3 with Heterogeneity 1 and $\tilde{k} = 10^{-4}$, the time to reach equilibrium are $t = 217, 156$ and 131 in main domain Ω_1 and $t = 578{,}513$ and 452 in Ω_2 (inclusions). The time is larger for subdomain Ω_2, where we have a smaller diffusion and expansion rate for Heterogeneity 1. For Heterogeneity 2, we observe opposite behavior with $t = 597{,}640$ and 655 in Ω_1 and $t = 247{,}312$ and 345 in Ω_2 (inclusions) for Geometry 1, 2 and 3, respectively. However, the time to reach equilibrium depends on the subdomain volume with smaller diffusion and expansion rate. We have a larger time for Geometry 2 (20% of domain filled with inclusion) and 3 (10% of domain filled with inclusion), and almost the same time for Geometry 1, where we have 44% of domain filled with inclusion. Moreover, we observe that more significant diffusion gives a shorter time to reach equilibrium, where results for $\tilde{k} = 10^{-6}$ are almost equal to the solution without diffusion (ODE).

Next, we present results for $\tilde{r} = 0.1, 0.08$ and 0.06 for $\tilde{k} = 10^{-4}$ and $u_0 = 0.5$. The results are shown in Figure 4.8 for two heterogeneity cases in Geometry 1, 2, and 3. Similarly to the homogeneous case, we observe a larger time to reach equilibrium for the lower expansion rate. Furthermore, the larger time is associated with the subdomain with a lower expansion rate (Ω_2 for Heterogeneity 1 and Ω_1 for Heterogeneity 2).

In Figure 4.9, we represent the influence of the initial condition on time to reach equilibrium. We simulate with $u_0 = 0.1, 0.4, 0.5, 0.6$ and 0.8 for fixed diffusion and expansion rate coefficients, $\tilde{k} = 10^{-4}$ and $\tilde{r} = 0.1$. Similarly to the homogeneous case, we obtain a larger time for a larger distance from the initial condition to the final equilibrium state for all Geometries. Moreover, we observe a larger time for Geometry 1 with larger inclusions than for geometries with smaller inclusions. For example, for Heterogeneity 1 we have $t = 746, 650$ and 563 in subdomain Ω_2 for Geometries 1, 2 and 3, respectively. We also observe larger time related to the larger volume of the subdomain with lower diffusion and expansion rate, where we have $t = 856, 833$ and 777 in subdomain Ω_1 with Heterogeneity 2 for Geometries 1, 2, and 3.

4.0.2 Two-Species Model

For the two-species model, we consider heterogeneous and homogeneous cases

- Heterogeneous case, where inclusions have a lower diffusion and lower expansion rate:

$$k_1(x) = \begin{cases} \tilde{k}/100, & x \in \Omega_1, \\ \tilde{k}, & x \in \Omega_2, \end{cases} \quad r_1(x) = \begin{cases} \tilde{r}/10, & x \in \Omega_1, \\ \tilde{r}, & x \in \Omega_2, \end{cases},$$

$$k_2(x) = \begin{cases} \tilde{k}, & x \in \Omega_1, \\ \tilde{k}/100, & x \in \Omega_2, \end{cases} \quad r_2(x) = \begin{cases} \tilde{r}, & x \in \Omega_1, \\ \tilde{r}/10, & x \in \Omega_2, \end{cases},$$

$$\alpha_{12}(x) = \begin{cases} \tilde{\alpha}, & x \in \Omega_1, \\ \tilde{\alpha}/5, & x \in \Omega_2, \end{cases}, \quad \alpha_{21}(x) = \begin{cases} \tilde{\alpha}/5, & x \in \Omega_1, \\ \tilde{\alpha}, & x \in \Omega_2, \end{cases}$$

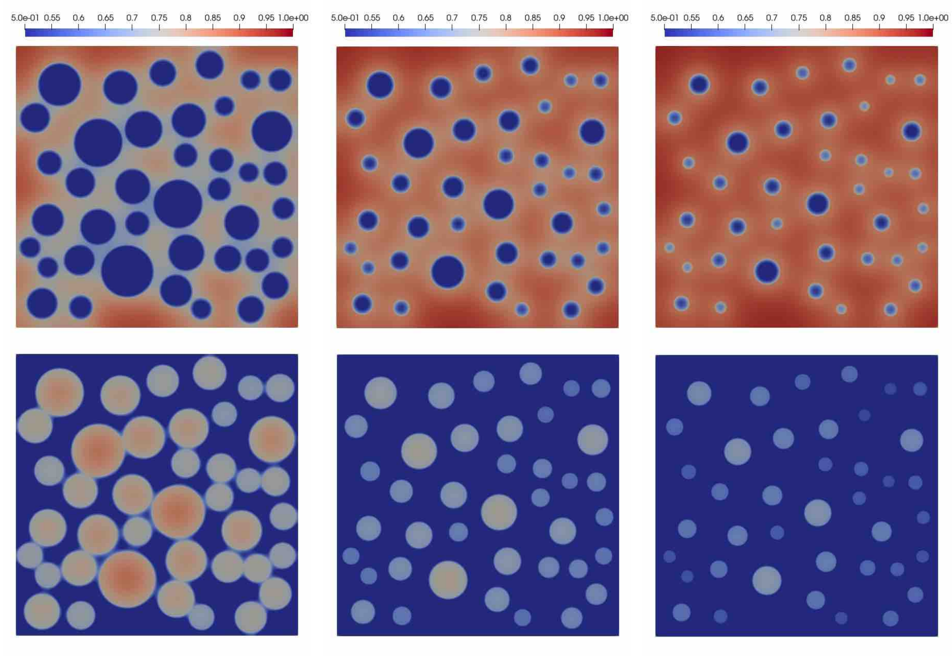

(a) Geometry 1 (b) Geometry 2 (c) Geometry 3

Figure 4.10: Two-species model. Heterogeneous case. Solution at the final time. First row: first species, $u^{(1)}$. Second row: second species, $u^{(2)}$

- Homogeneous case, where we set the same coefficients in the main domain and inclusions:

$$k = \tilde{k}, \quad r = \tilde{r}, \quad \alpha_{12} = \alpha_{21} = \tilde{\alpha}, \quad x \in \Omega.$$

We note that the coefficients for the second species are opposite to the first species coefficients. Therefore, we consider one heterogeneity case for the two-species model because the opposite heterogeneity case, similar to the heterogeneous domain 2 in the one-species model, gives an identical model with the same results.

We calculate the average population of each species in Ω_1 and Ω_2

$$\bar{u}^{(\zeta)}(t) = \frac{1}{|\Omega_1|} \int_{\Omega_1} u^{(\zeta)}(x,t)\, dx,$$

where $|\Omega|$ is the volume of the domain Ω, simulations are performed for 4,000 time layers. The time to reach equilibrium is calculated using difference between solution on current and previous time layer, $|\bar{u}^{(k)} - \check{\bar{u}}^{(k)}| < \epsilon$ with $\epsilon = 10^{-5}$ for each k.

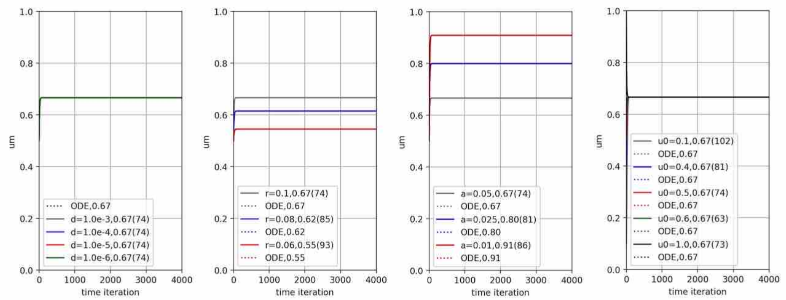

(a) $u^{(1)} \in \Omega$.

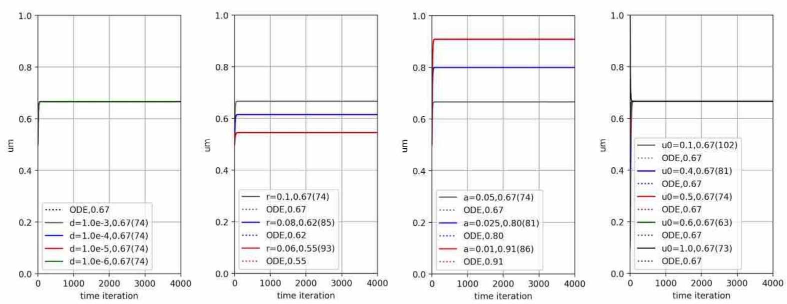

(b) $u^{(2)} \in \Omega$.

Figure 4.11: Two-species model. Homogeneous case. Effect of diffusion, expansion rate, competition term and initial condition (from left to right).

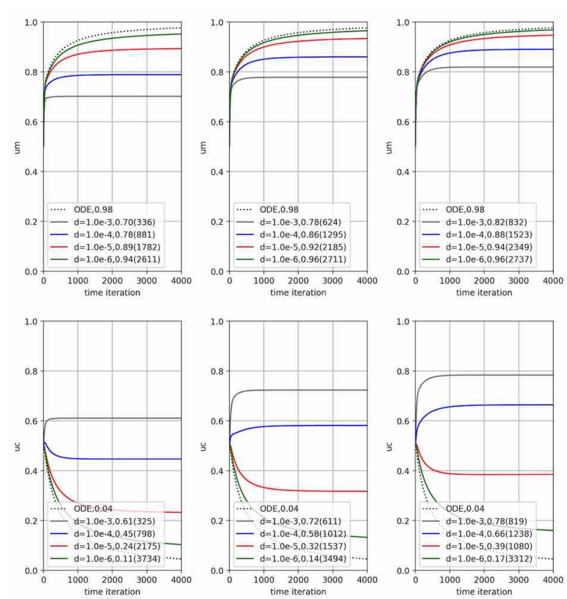

(a) $u^{(1)}$ in Geometry 1, 2 and 3 (from left to right)

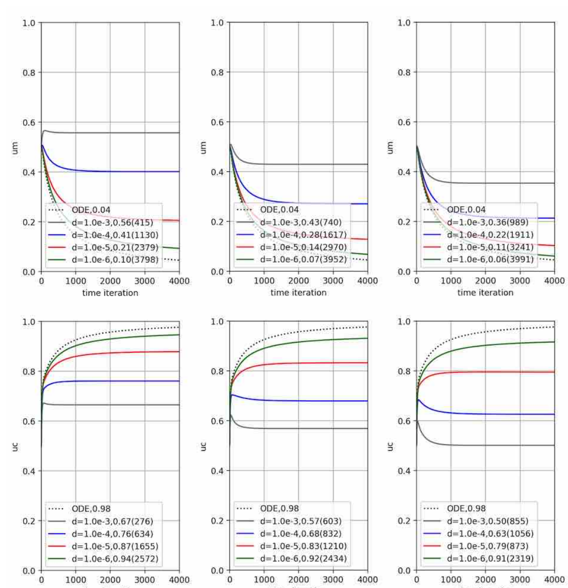

(b) $u^{(2)}$ in Geometry 1, 2 and 3 (from left to right)

Figure 4.12: Two-species model. Effect of diffusion. First row: $u_m^{(\zeta)} \in \Omega_1$. Second row: $u_c^{(\zeta)} \in \Omega_2$

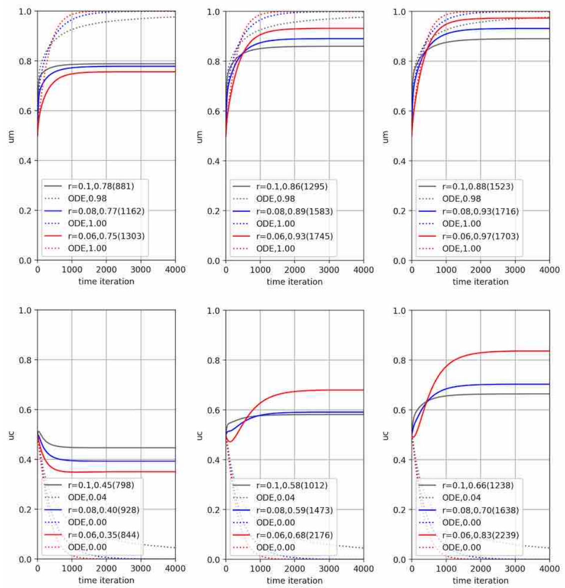

(a) $u^{(1)}$ in Geometry 1, 2 and 3 (from left to right)

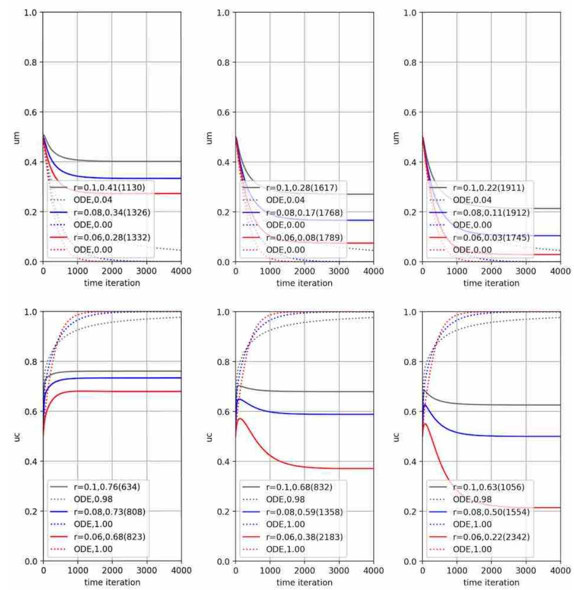

(b) $u^{(2)}$ in Geometry 1, 2 and 3 (from left to right)

Figure 4.13: Two-species model. Effect of expansion rate. First row: $u_m^{(\zeta)} \in \Omega_1$. Second row: $u_c^{(\zeta)} \in \Omega_2$

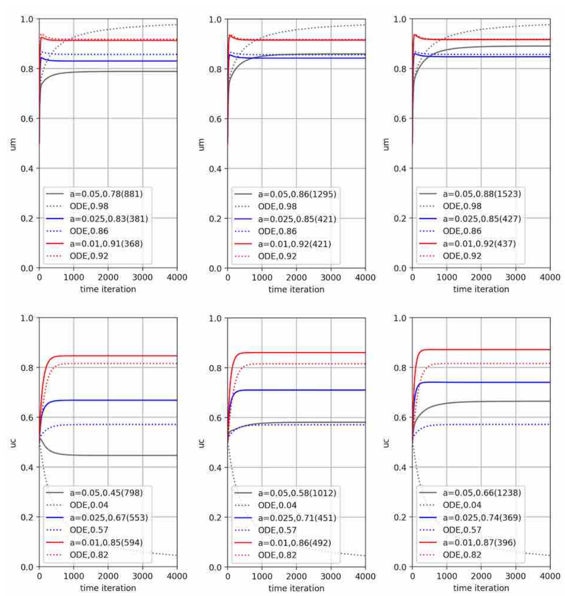

(a) $u^{(1)}$ in Geometry 1, 2 and 3 (from left to right)

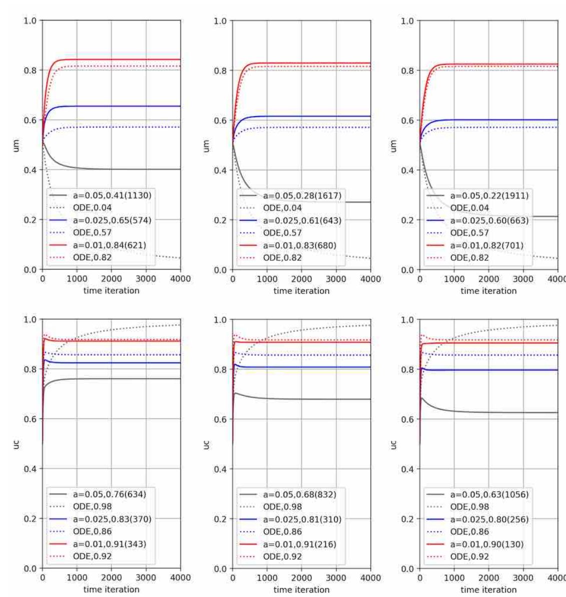

(b) $u^{(2)}$ in Geometry 1, 2 and 3 (from left to right)

Figure 4.14: Two-species model. Effect of competition coefficient. First row: $u_m^{(\zeta)} \in \Omega_1$. Second row: $u_c^{(\zeta)} \in \Omega_2$

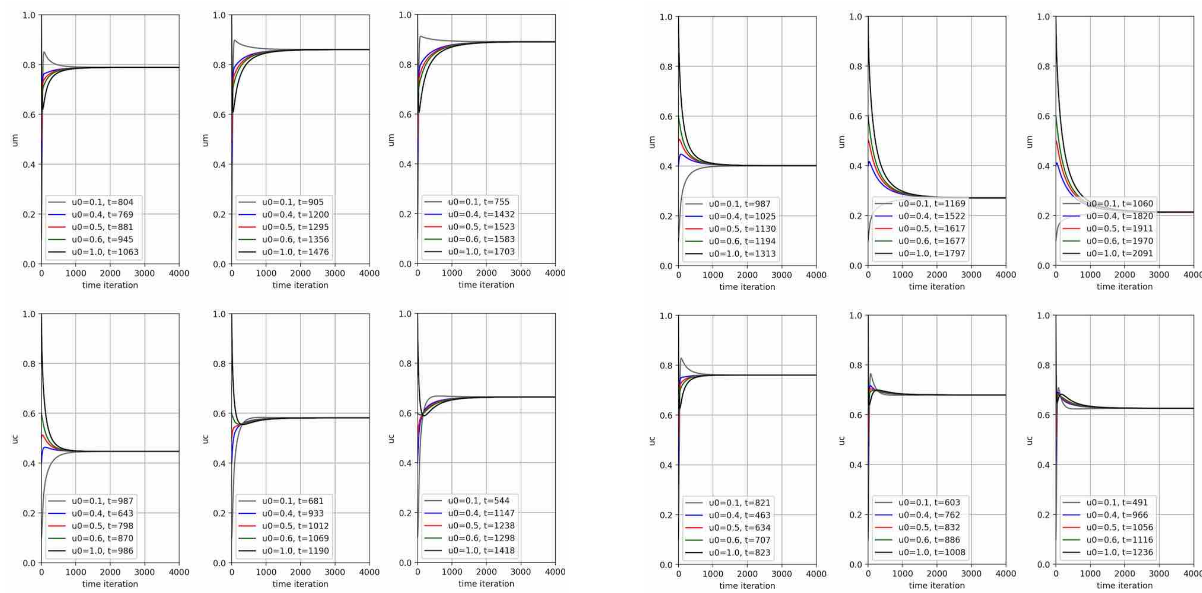

(a) $u^{(1)}$ in Geometry 1, 2 and 3 (from left to right) (b) $u^{(2)}$ in Geometry 1, 2 and 3 (from left to right)

Figure 4.15: Two-species model. Effect of initial conditions. First row: $u_m^{(\zeta)} \in \Omega_1$. Second row: $u_c^{(\zeta)} \in \Omega_2$

Solution at three time layers $t = 40, 100$, and 200 for two-species model is presented in Figure 4.10 for Geometry 1,2,and 3. Results are presented for $\tilde{k} = 10^{-4}$, $\tilde{\alpha} = 0.05$ and $\tilde{r} = 0.1$. We observe the effect of the radius of the inclusion into the final equilibrium state. For time and final equilibrium state, we obtain

- Geometry 1:

$$(u_m^{(1)}, u_m^{(2)}) = (0.78, 0.41) \in \Omega_1, \quad \text{with} \quad (t_m^{(1)}, t_m^{(2)}) = (881, 1130),$$

$$(u_c^{(1)}, u_c^{(2)}) = (0.45, 0.76) \in \Omega_2 \quad \text{with} \quad (t_c^{(1)}, t_c^{(2)}) = (798, 634).$$

- Geometry 2:

$$(u_m^{(1)}, u_m^{(2)}) = (0.86, 0.28) \in \Omega_1, \quad \text{with} \quad (t_m^{(1)}, t_m^{(2)}) = (1295, 1617),$$

$$(u_c^{(1)}, u_c^{(2)}) = (0.58, 0.68) \in \Omega_2 \quad \text{with} \quad (t_c^{(1)}, t_c^{(2)}) = (1012, 832).$$

- Geometry 3:

$$(u_m^{(1)}, u_m^{(2)}) = (0.88, 0.22) \in \Omega_1, \quad \text{with} \quad (t_m^{(1)}, t_m^{(2)}) = (1523, 1911),$$

$$(u_c^{(1)}, u_c^{(2)}) = (0.66, 0.63) \in \Omega_2 \quad \text{with} \quad (t_c^{(1)}, t_c^{(2)}) = (1238, 1056).$$

Here $u_m^{(\zeta)}$ and $u_c^{(\zeta)}$ are the time to reach equilibrium for species $\zeta = 1,2$ in domain Ω_1 and Ω_2. The larger time to reach equilibrium is obtained in Geometry 3 for both species and subdomains. For Geometry 3, we also observe a larger final population for first species ($u_m^{(1)}$ and $u_c^{(1)}$) and smaller population for second species ($u_m^{(2)}$ and $u_c^{(2)}$)

Results for the Homogeneous case in represented in Figure 4.11. We observe a same final population for both species, $u^{(1)} = u^{(2)} = 0.67$ with $t = 74$. We observe that solution does not depend on the diffusion rate for the homogeneous case. Similarly to the one-species model, we obtain a smaller population with a larger time for a lower expansion rate. The time to reach equilibrium depends on the distance from the initial condition to the final state, where we obtain a larger time to reach equilibrium for a larger distance.

The time to reach equilibrium for different diffusion coefficients $\tilde{k} = 10^{-3}, 10^{-4}, 01^{-5}$ and 10^{-6} is presented in Figure 4.12 for Geometry 1,2 and 3 with heterogeneous properties. The expansion rate and initial condition are fixed $\tilde{r} = 0.1$ and $u_0 = 0.5$. The ODE solution is also depicted by black dotted lines in each figure to highlight the effect of the diffusion into the solution. We observe a larger time to reach equilibrium in Geometry 3 for $\tilde{d} = 10^{-4}$. However, for $\tilde{d} = 10^{-6}$, we have a larger time for the first species in Geometry 1. For each geometry time to reach equilibrium is increases when the diffusion coefficient decreases.

Next, we present results for $\tilde{r} = 0.1, 0.08$ and 0.06 for $\tilde{k} = 10^{-4}$, $\tilde{a} = 0.05$, and $u_0 = 0.5$. The results are shown in Figure 4.13 for two heterogeneity cases in Geometry 1, 2, and 3. Similarly to the homogeneous case, we observe a larger time to reach equilibrium for the lower expansion rate. The solution is represented with ODE solution (without diffusion). Compared with the ODE solution, we observe that the size of the inclusions significantly impacts the final solution due to the diffusion. Furthermore, the effect is dramatic for inclusions subdomain Ω_2. In Figure 4.14, we present results for different competition coefficients, $\tilde{a} = 0.05, 0.025, 0.01$ with fixed $\tilde{k} = 10^{-4}$, $\tilde{r} = 0.1$ and $u_0 = 0.5$. Similarly to varying values $\tilde{r}$, we observe a huge impact of the parameters on solution inside inclusions due to diffusion.

In Figure 4.15, we represent the influence of the initial condition on time to reach equilibrium. We simulate with $u_0 = 0.1, 0.4, 0.5, 0.6$ and 0.8 for fixed diffusion and expansion rate coefficients, $\tilde{k} = 10^{-4}$, $\tilde{a} = 0.05$ and $\tilde{r} = 0.1$. We observe that the initial condition does not affect the final equilibrium state.

4.1 Numerical Solution of the Spatial-Temporal Model of Population Distribution in Heterogeneous Domain

Coastal swamps are virtual environments that advantage human wellbeing and prosperity, counting securing inland ranges from storm surges, putting away water, expelling supplements from watersheds, and giving nursery environments for essential commercial and recreational fisheries. The approach is to create a determining show for changes in a plant to create an estimating show of changes in a plant to decide the impacts of human exercises on bog structure and work, specifically swamp vegetation. Asset supervisors might utilize the show to decide how much water to redirect back into the swamp to extend water levels to reestablish the vegetated wetlands. This data can assess the costs and benefits of different rebuilding scenarios. In addition, the mathematical show may well be altered as required and connected to swamps in other districts of the nation that are vulnerable to the adverse environmental and natural effects of development and water asset development.

4.1.1 Mathematical Model

The mathematical model is described by the following parabolic equation with nonlinear right hand side

$$\frac{\partial u}{\partial t} - \nabla \cdot (k(x) \nabla u) = r(x)(1-u)u, \quad x \in \Omega, \quad 0 < t < T, \tag{4.15}$$

where $u = u(x,t)$ if the population of the species at time t, r is the expansion rate and k is the diffusion coefficient. We consider equation (4.15) in the two- dimensional heterogeneous domain $\Omega = \Omega_1 \cup \Omega_2$, where Ω_1 is the main domain and Ω_2 is the subdomain 4.16 related to the inclusions.

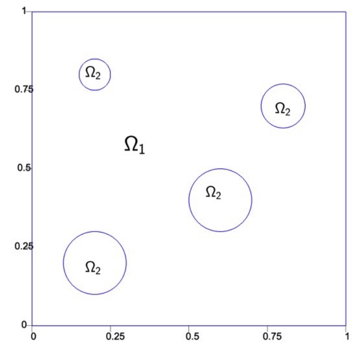

Figure 4.16: Illustration of the heterogeneous domain, $\Omega = \Omega_1 \cup \Omega_2$.

For the equation parameters, we set

$$k(x) = \begin{cases} k_1, & x \in \Omega_1, \\ k_2, & x \in \Omega_2, \end{cases} \quad r(x) = \begin{cases} r_1, & x \in \Omega_1, \\ r_2, & x \in \Omega_2, \end{cases}$$

We set the initial condition

$$u = u_0, \quad x \in \Omega, \quad t = 0, \tag{4.16}$$

and the boundary conditions are as follows:

$$u = 0, \quad x \in \Gamma_1, \quad -k\frac{\partial u}{\partial n} = 0, \quad x \in \Gamma_2, \quad 0 < t < T, \tag{4.17}$$

where $\partial\Omega = \Gamma_1 \cup \Gamma_2$.

4.1.2 Approximation using Finite Element Method

For numerical solution of the initial - boundary value problem (4.15) - (4.17), we use a Finite Element Method for approximation by space. To approximate given parabolic equation, we use the following finite difference approximation for time derivative

$$\frac{\partial u}{\partial t} \approx \frac{u^{n+1} - u^n}{\tau},$$

where τ is the given time step and $u^n = u(x,t^n)$, $\tau = T/N$, N is the number of time steps, n is the time layer, $n = 1,2,\ldots,N$. For initial condition, we have $u^0 = u_0$. Let $V = \{v \in H^1(\Omega) : v = 0,\ x \in \Gamma_1\}$. where $H^1(\Omega)$ is the Sobolev space containing functions v such that v^2 and $\left|\nabla v^2\right|$ have finite integrals over Ω. To write a variational formulation of the problem, we multiply the equation (4.15) by the test function v and integrate over the domain Ω. Using integration-by-parts formula

$$-\int_\Omega \nabla \cdot (k(x)\nabla u)\ v\ dx = \int_\Omega k(x)\nabla u \cdot \nabla v\ dx - \int_{\partial\Omega} k(x)\frac{\partial u}{\partial \nu}\ v\ ds$$

where ν is the unit vector to the boundary $\partial\Omega$. After applying boundary conditions (4.17), we have the following variational formation: find $u \in V$ such that

$$\int_\Omega \frac{u^{n+1} - u^n}{\tau}\ v\ dx - \int_\Omega k(x)\nabla u^{n+1} \cdot \nabla v\ dx = \int_\Omega r(x) u^{n+1}(1-u^n)\ v\ dx, \quad \forall v \in V.$$

We note that, we used a explicit-implicit time approximation. Next, we rewrite vatiational formulation in the following form: find $u \in V$ such that:

$$a(u^{n+1}, v) = L(v), \quad \forall v \in\ V,$$

where bilinear and linear forms are defined as follows

$$a(u,v) = \frac{1}{\tau}\int_\Omega u\ v\ dx + \int_\Omega k(x)\nabla u \cdot \nabla v\ dx + \int_\Omega r(x)u(1-u^n)\ v\ dx,$$

$$L(v) = \frac{1}{\tau}\int_\Omega u^n\ v\ dx.$$

Let $\mathcal{T}^h$ be a partition of the domain Ω that resolve inclusions on the grid level 4.17 with mesh

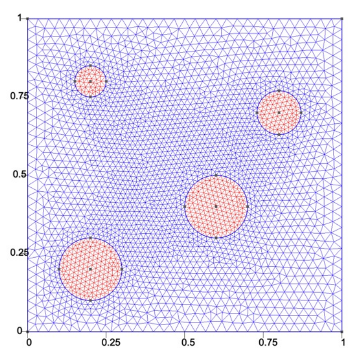

Figure 4.17: Illustration of the computational mesh with triangular cells, $\mathcal{T}^h$.

size h. Let $V_h \subset V$ contains functions which are piecewise linear in each fine-grid element K. Therefore, we have following discrete variational formulation: find $u_h \in V_h$ such that

$$a(u_h^{n+1}, v) = L(v), \quad \forall v \in\ V,$$

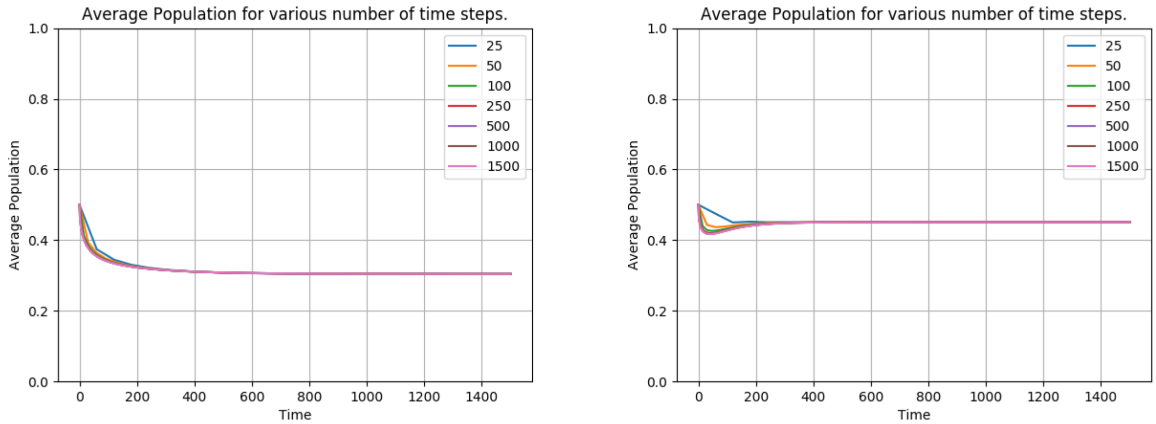

Figure 4.18: Case 1 (N): $k = 10^{-3}$, $r = 0.01$,and $u = 0.5$

We can write the above discrete systems in the matrix form as follows

$$A_h U_h^{n+1} = F_h^u, \tag{4.18}$$

where

$$U_h^{n+1} = [u_j^{n+1}], \quad A_h = [a_{ij} = a(\psi_i, \psi_j)], \quad F_h^u = [f_j = l_u(\psi_j)],$$

with linear basis function $\psi_i \in \mathbb{P}_1$. The size of the discrete system is $DOF = N_h$, where N_h is the number of fine grid nodes. Finally, we have the following algorithm:

- Set initial condition $u_h^n = u_0$ for $n = 0$.

- For $n = 1,2,...$, we solve system of linear equations (4.18) to find U_h^{n+1} for given solution from previous time step U_h^n.

4.1.3 Influence of Parameters to Average Solution vs Time

We simulate with $T = 1500$ and set initial conditions $u_0 = 0.5$. We consider two test cases:

- Homogeneous domain $k_1 = k_2$ and $r_1 = r_2$.

- Heterogeneous domain with $k_2 = 0.1$ and $r_2 = 0.1$.

We solve problem in domain $\Omega = [0,1]^2$ with 4 circle inclusions. Computational mesh contains 3183 nodes and 6244 triangular cells. Here we use a linear basis functions and number of unknowns is equals to the number of mesh nodes, $N = 3183$.

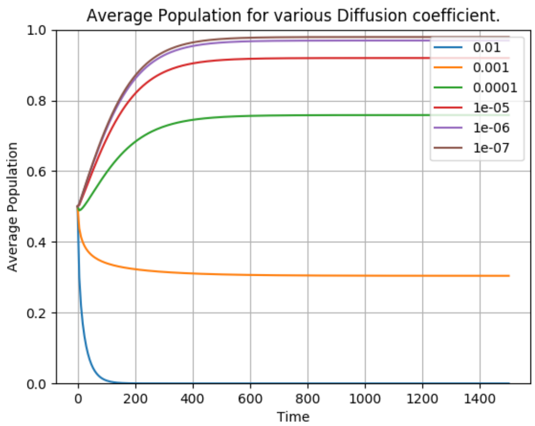

Figure 4.19: Case 2 (k): $N = 250$, $r = 0.01$ and $u = 0.5$

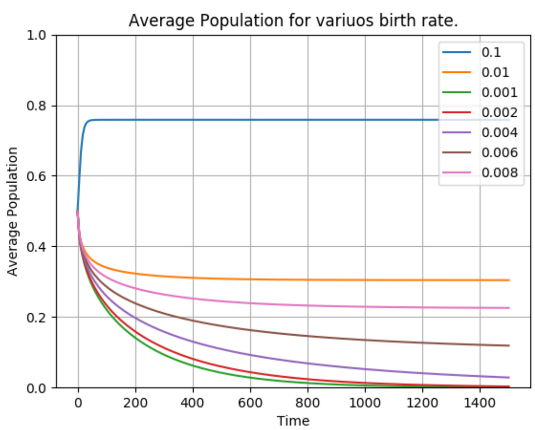

Figure 4.20: Case 3 (r): $k = 0.001$ and $N = 250$,$u = 0.5$.

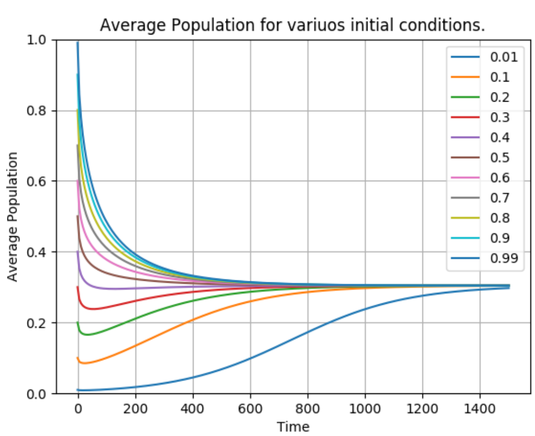

Figure 4.21: Case 4 (u_0): $k = 0.001$, $r = 0.01$ and $N = 250$.

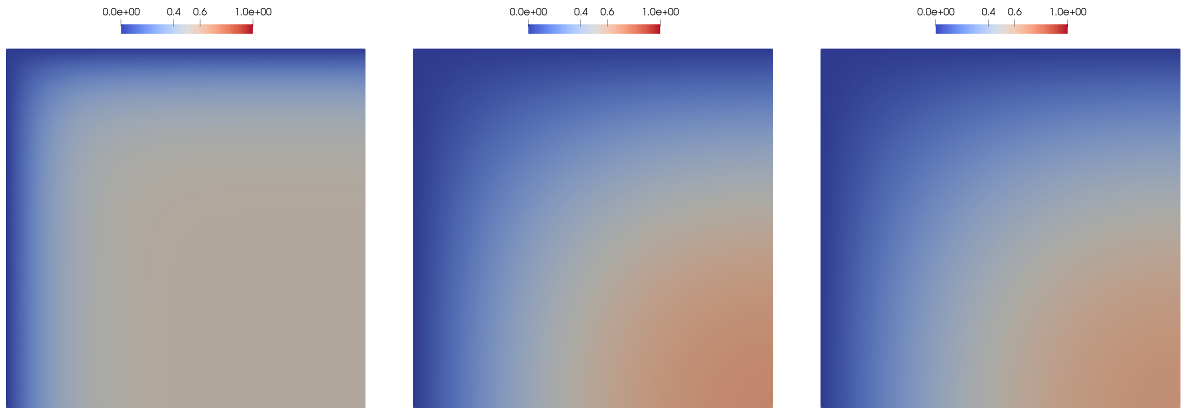

Figure 4.22: Homogeneous case. $k = 10^{-3}$, $r = 0.01$. $n = 1,25,250$

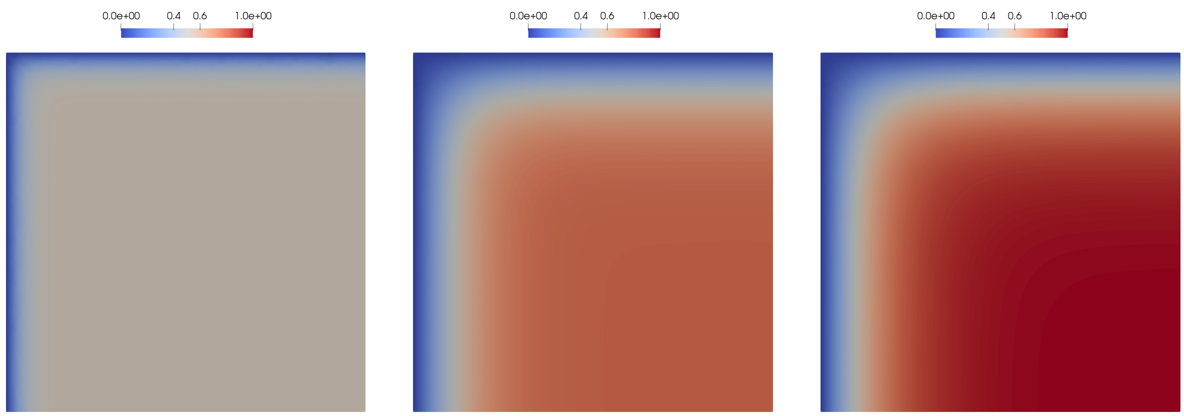

Figure 4.23: Homogeneous case. $k = 10^{-4}$, $r = 0.01$. $n = 1,25,250$

- Numerical implementation is based on the open-source finite element library FEniCS.

- For geometry and mesh construction, we use Gmsh program.

- The Paraview program is used for visualization.

- In figures 4.18,4.19, 4.20, 4.21, left pictures represents Homogeneous case and right heterogeneous case.

4.1.4 Numerical Solutions for Different Times

The results of this chapter demonstrate the important influence of domain heterogeneity and parameter modifications on the dynamics of the mathematical model simulating the behaviour of biological organisms. For various geometries, the one-species model displayed unique behaviour, with changes in the time to reach equilibrium associated with the percentage of the domain filled

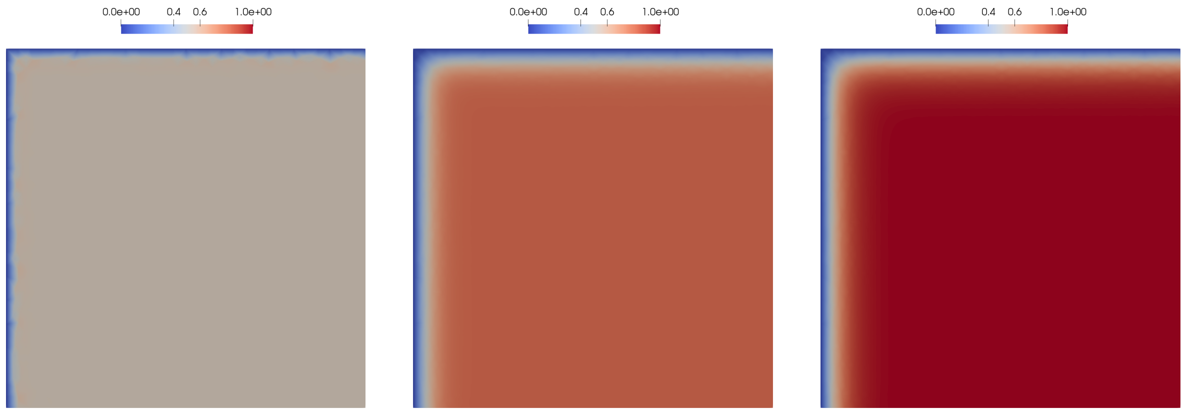

Figure 4.24: Homogeneous case. $k = 10^{-5}$, $r = 0.01$. $n = 1,25,250$

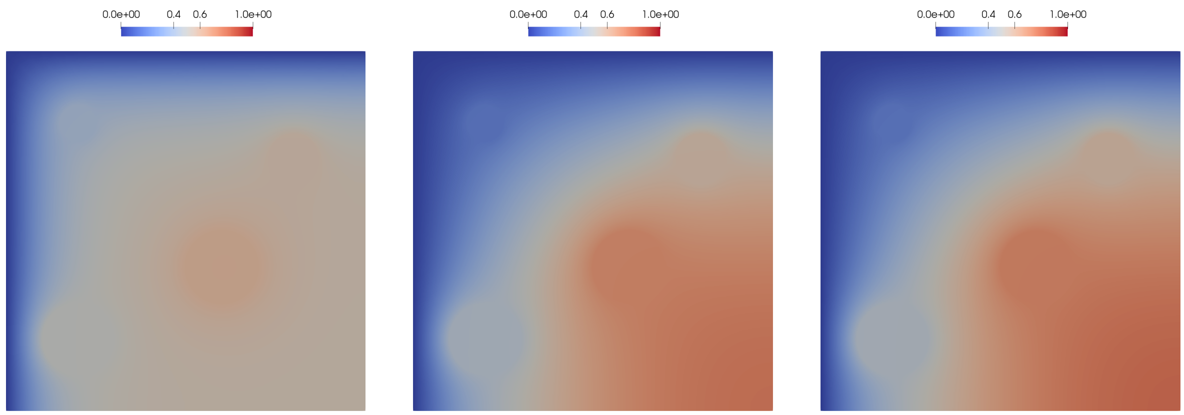

Figure 4.25: Heterogeneous case. $k = 10^{-3}$, $r = 0.01$. $n = 1,25,250$

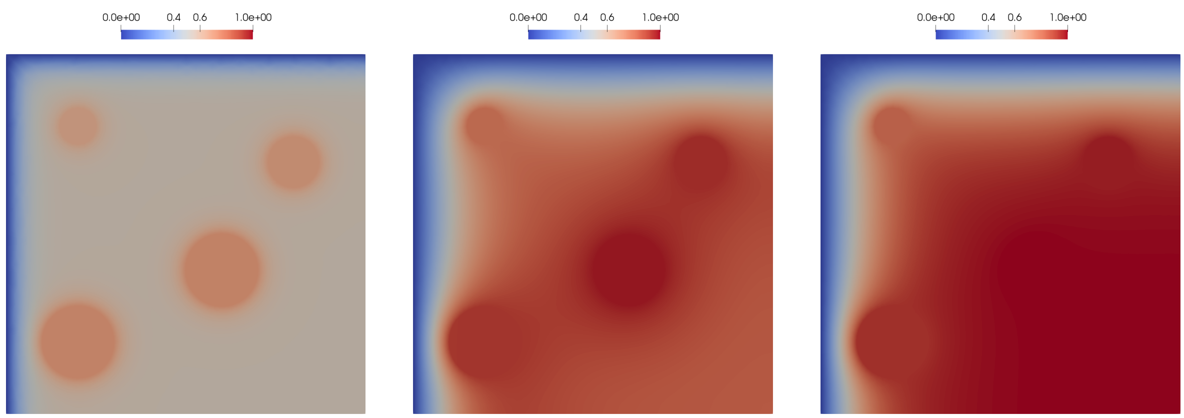

Figure 4.26: Heterogeneous case. $k = 10^{-3}$, $r = 0.01$. $n = 1,25,250$

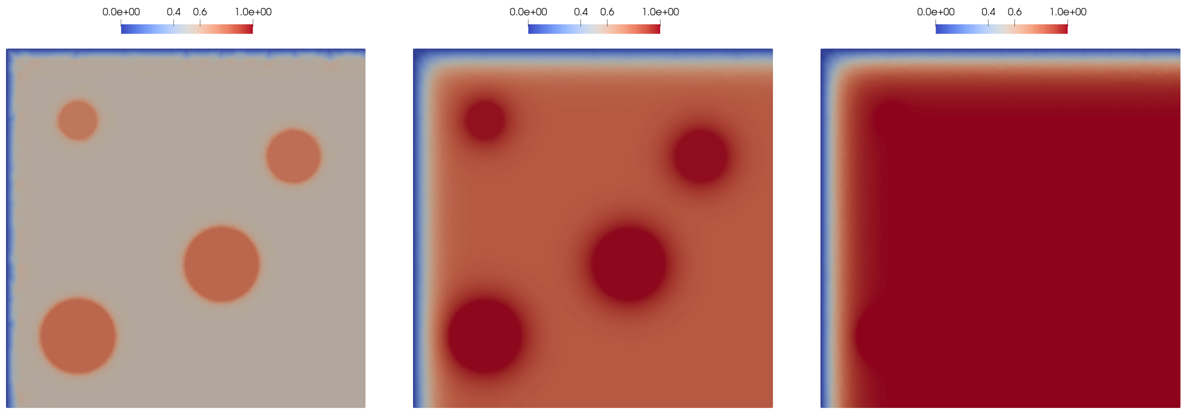

Figure 4.27: Heterogeneous case. $k = 10^{-3}$, $r = 0.01$. $n = 1{,}25{,}250$

by inclusions. The two-species model, in contrast, showed interesting interactions between the opposing species and their reactions to heterogeneity. The simulations clarified how diffusion and expansion rates affect the equilibrium state. Additionally, the impact of the initial conditions was looked at, emphasising how little of an impact they had on the ultimate balance. With possible implications for ecological studies, the findings of this investigation offer valuable insights into the underlying mechanisms driving species dynamics in varied habitats.

CHAPTER 5: MATHEMATICAL MODEL WITH FRACTIONAL-TIME

The use of time-fractional diffusion-reaction equations as effective tools for analysing population dynamics in heterogeneous environments is explored in this chapter. Our main concern is a one-species model that depicts how a population changes over time. Diffusion, which indicates the dispersion of people, and reaction terms, which take birth and death into account, are both included in the fundamental equation. The diffusion coefficient, which measures the degree of dispersal, and the expansion rate, which controls population growth or fall, both have a significant impact on the dynamics of the population. We also examine the effects of domain heterogeneity, which is a division of the environment into distinct areas with different characteristics. We obtain significant r esultsinto h ow t hese e lements c ombine t o a ffect t he b ehaviour o f t he p opulation by running extensive numerical simulations on various test geometries. Our studies provides important information for ecological modelling and future study by shedding light on the complexity of ecological systems in many difficult situations.

- Diffusion-reaction equation for $u(x,t)$ $(0 < \alpha \leq 1)$

$$\frac{\partial^{\alpha} u}{\partial t^{\alpha}} - \nabla \cdot (k(x) \nabla u) = r(x)(1-u)u, \quad x \in \Omega, \quad 0 < t < T,$$

where $u(x,t)$ is the population of the species at time t, r is the expansion rate and k is the diffusion coefficient. The Caputo derivative of the order α

$$\partial_t^{\alpha} u(t) = \frac{1}{\Gamma(1-\alpha)} \int_0^t (t-s)^{-\alpha} \frac{\partial u}{\partial s}(s) ds, \quad 0 < \alpha \leq 1.$$

Let $\Omega = \Omega_1 \cup \Omega_2$ be the heterogeneous domain. We set

$$k(x) = \begin{cases} k_1, & x \in \Omega_1, \\ k_2, & x \in \Omega_2, \end{cases} \qquad r(x) = \begin{cases} r_1, & x \in \Omega_1, \\ r_2, & x \in \Omega_2, \end{cases}$$

where Ω_1 be the main domain and Ω_2 be the subdomain related to the inclusions. Let N be the number of time steps, τ be the given time step, $\tau = T/N$, $u^n = u(x,t^n)$, n is the time layer, $n = 1,2,\ldots,N$. The fractional-order derivative of the fucntion u^n is defined using the following

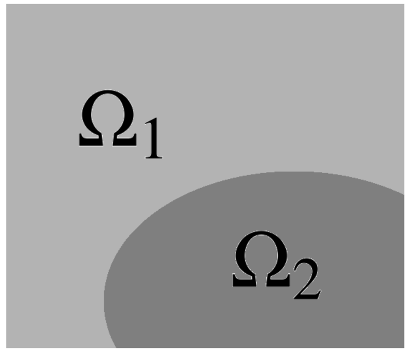

Figure 5.28: Heterogeneous Domain $\Omega = \Omega_1 \cup \Omega_2$

formula:

$$\frac{\partial^\alpha u^n}{\partial t^\alpha} \approx \zeta_\tau^{(\alpha)} \left(u^n - u^{n-1} + \sum_{j=2}^{n} \zeta_{j-1}^{(\alpha)} (u^{n-j+1} - u^{n-j}) \right),$$

where

$$\zeta_\tau^{(\alpha)} = \frac{1}{\tau^\alpha \Gamma(2-\alpha)}, \quad \zeta_{j-1}^{(\alpha)} = j^{1-\alpha} - (j-1)^{1-\alpha}.$$

Discrete problem:

$$\zeta_\tau^{(\alpha_i)} \int_\Omega (u^{n+1} - u^n)\ v\ dx + \zeta_\tau^{(\alpha_i)} \sum_{j=2}^{n} \zeta_{j-1}^{(\alpha_i)} \int_\Omega (u_i^{n-j+1} - u_i^{n-j})\ v\ dx$$
$$- \int_\Omega k(x) \nabla u^{n+1} \cdot \nabla v\ dx = \int_\Omega r(x) u^n (1 - u^n)\ v\ dx,$$

where $\forall v \in V$, $V = H^1(\Omega)$.

5.1 Numerical Results for Time-Fractional Model

We consider three test geometries with small, medium and large inclusions:

- Geometry 1 with $|\Omega_1| = 0.56$ and $|\Omega_2| = 0.44$. 92,844 cells and 46,783 nodes.

- Geometry 2 with $|\Omega_1| = 0.8$ and $|\Omega_2| = 0.2$. 91,352 cells and 46,037 nodes.

- Geometry 3 with $|\Omega_1| = 0.9$ and $|\Omega_2| = 0.1$. 89,460 cells and 45,091 nodes. - Heterogeneity 1,

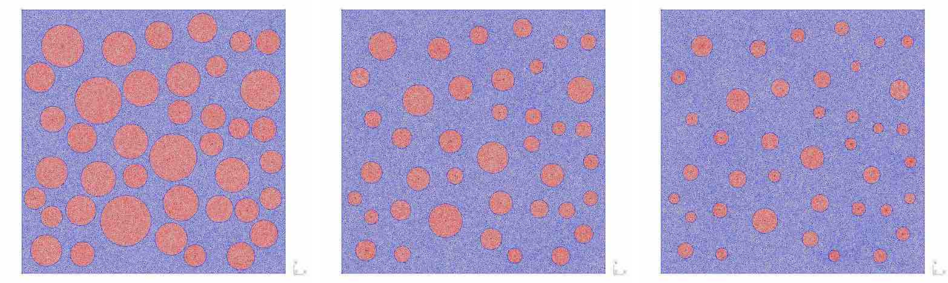

Figure 5.29: Geometries with Small, Medium and Large Inclusions

where inclusions have a smaller diffusion and smaller expansion rate:

$$k(x) = \begin{cases} \tilde{k}, & x \in \Omega_1, \\ \tilde{k}/100, & x \in \Omega_2, \end{cases} \qquad r(x) = \begin{cases} 1s\tilde{r}, & x \in \Omega_1, \\ \tilde{r}/10, & x \in \Omega_2, \end{cases}$$

- Heterogeneity 2, where main domain have a smaller diffusion and smaller expansion rate:

$$k(x) = \begin{cases} \tilde{k}/100, & x \in \Omega_1, \\ \tilde{k}, & x \in \Omega_2, \end{cases} \qquad r(x) = \begin{cases} \tilde{r}/10, & x \in \Omega_1, \\ \tilde{r}, & x \in \Omega_2, \end{cases}$$

Dynamic of the solution at three time layers $t = 40, 100$, and 200. $u_0 = 0.5$, $\tilde{k} = 10^{-4}$ and $\tilde{r} = 0.1$

Dynamic of the solution at three time layers $t = 40, 100$, and 200. $u_0 = 0.5$, $\tilde{k} = 10^{-4}$ and $\tilde{r} = 0.1$

- Effect of Fractional Time DerivativeFirst row: $u_m \in \Omega_1$. Second row: $u_c \in \Omega_2$. $\tilde{k} = 10^{-4}$, $\tilde{r} = 0.1$ and $u_0 = 0.5$.

- For smaller α we have slower dynamic with smaller average value for main domain and inclusions.

- We observe a huge effect of α to the time to reach equilibrium.

- Heterogeneity and Heterogeneity 2 have opposite behavior.

The outcomes of thorough numerical simulations performed on several test geometries with variable inclusion sizes are provided and thoroughly examined. We obtain essential facts into the impacts of fractional time derivatives, diffusion coefficients, expansion rates, and domain heterogeneity on the population dynamics by visualising the dynamic behaviour of the solution at various time layers. The findings are discussed in depth in the chapter's conclusion, with special attention paid to how important they are for understanding ecological systems in complicated contexts. With

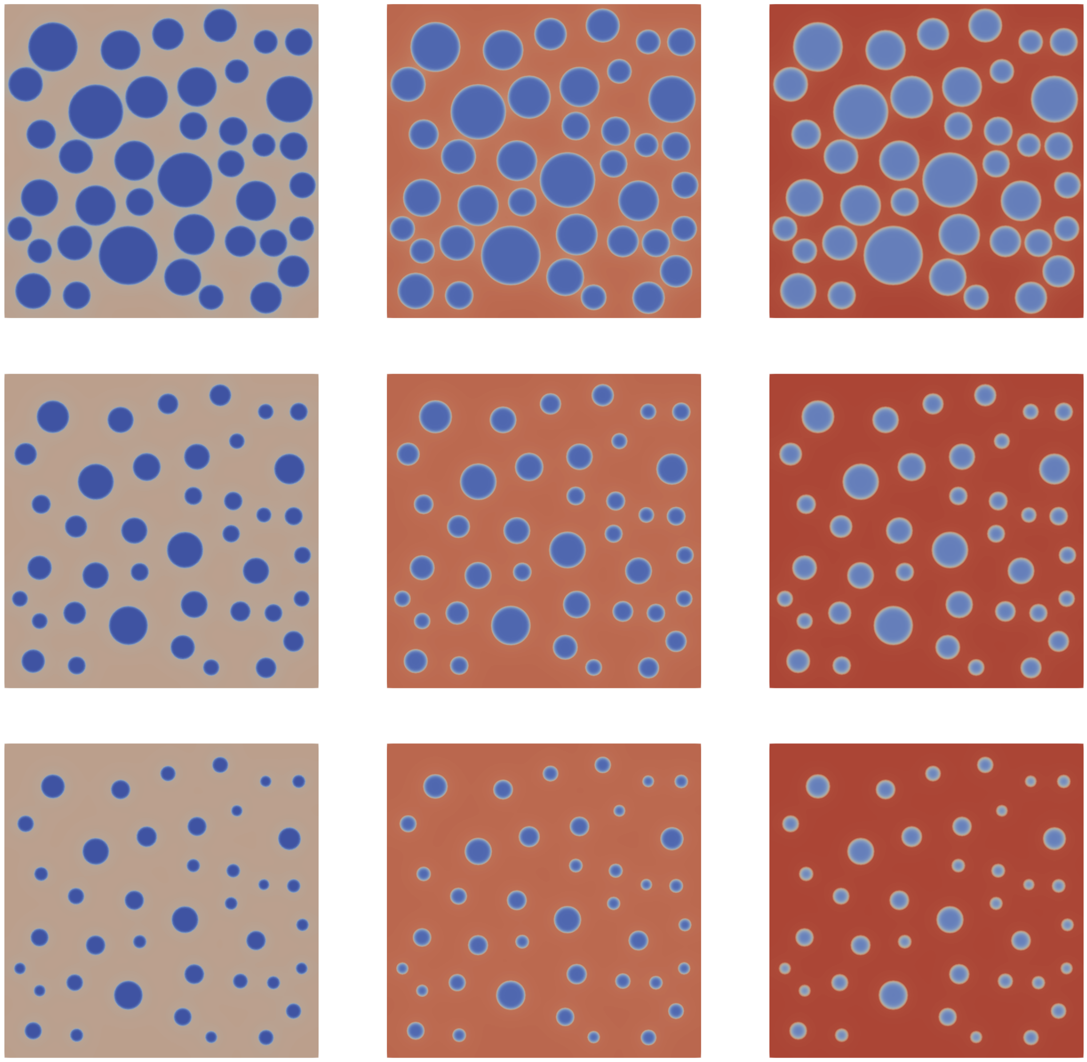

Figure 5.30: Heterogeneity 1 with $\alpha = 0.7$

this study, we hope to advance ecological modelling and stimulate further research in this dynamic and developing area.

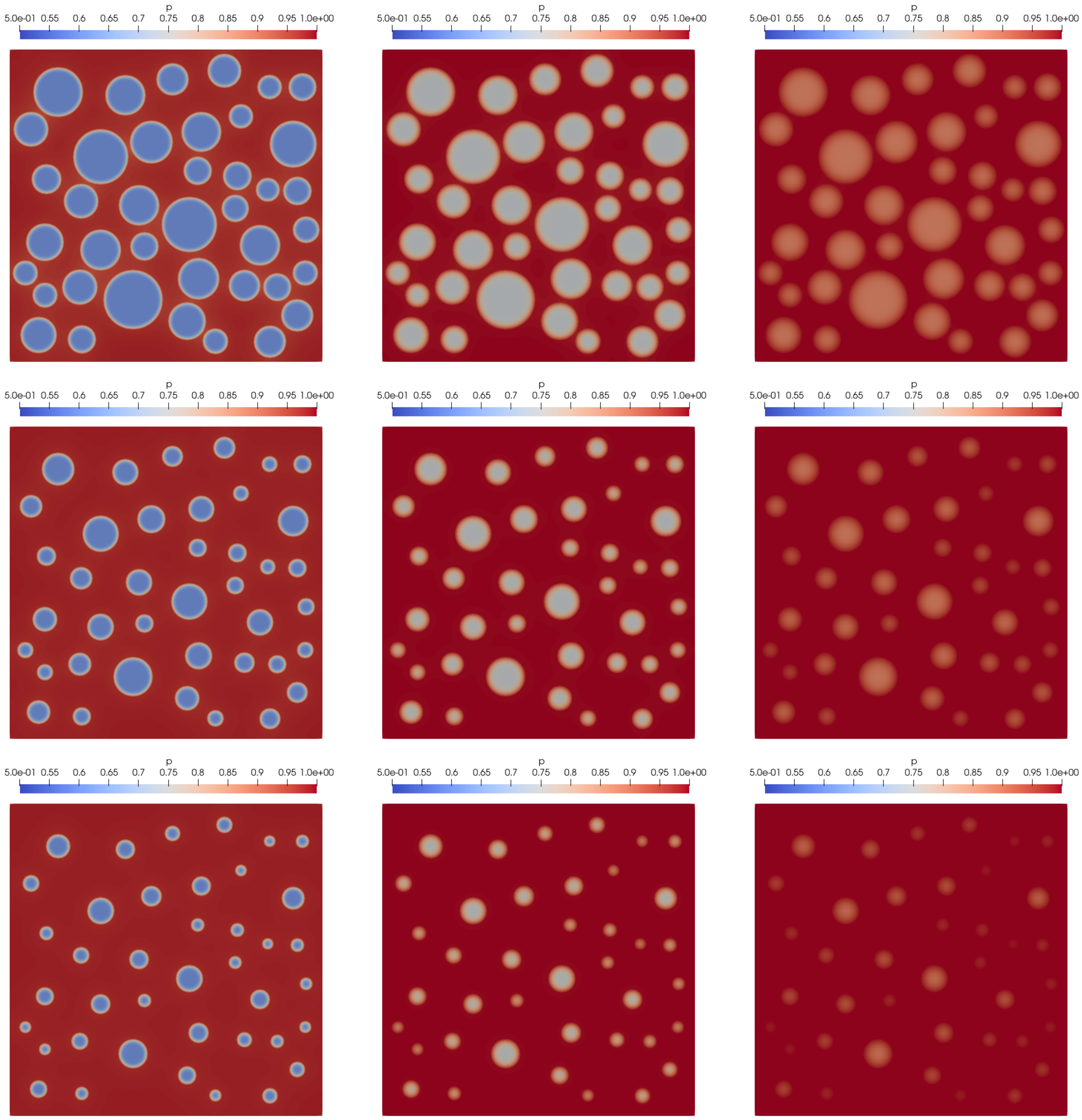

Figure 5.31: Heterogeneity 1 with α = 1

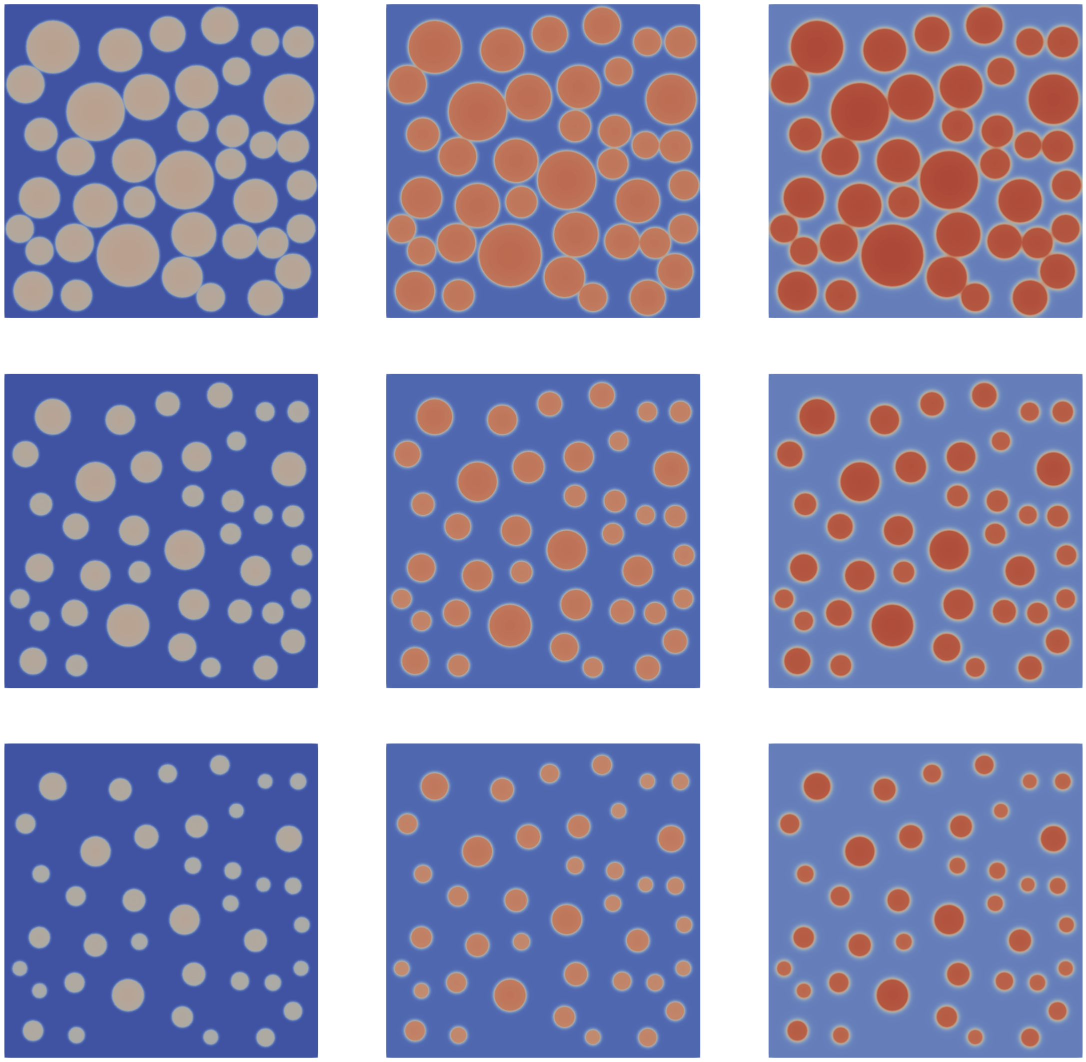

Figure 5.32: Heterogeneity 2 with $\alpha = 0.7$

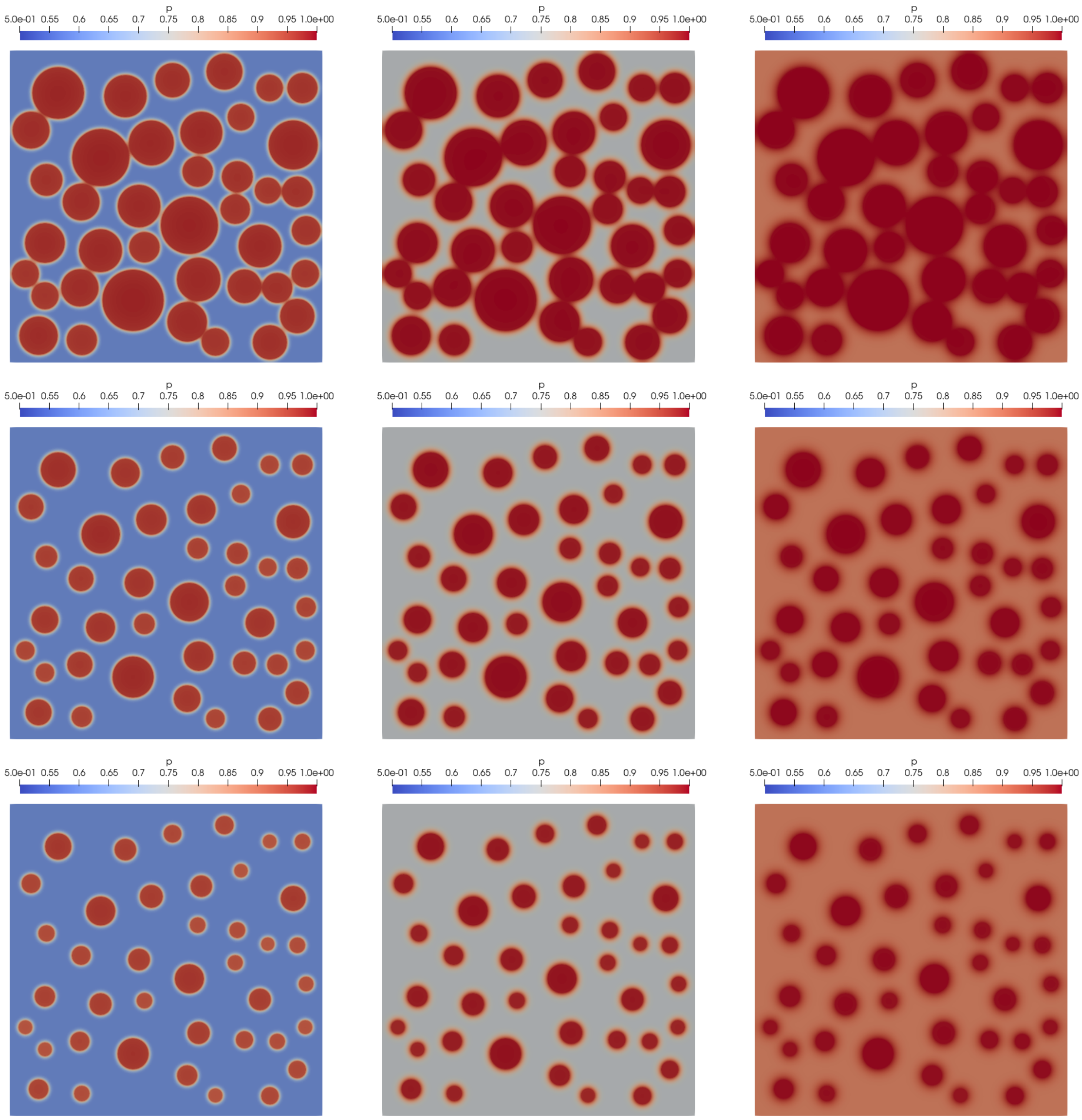

Figure 5.33: Heterogeneity 2 with $\alpha = 1$

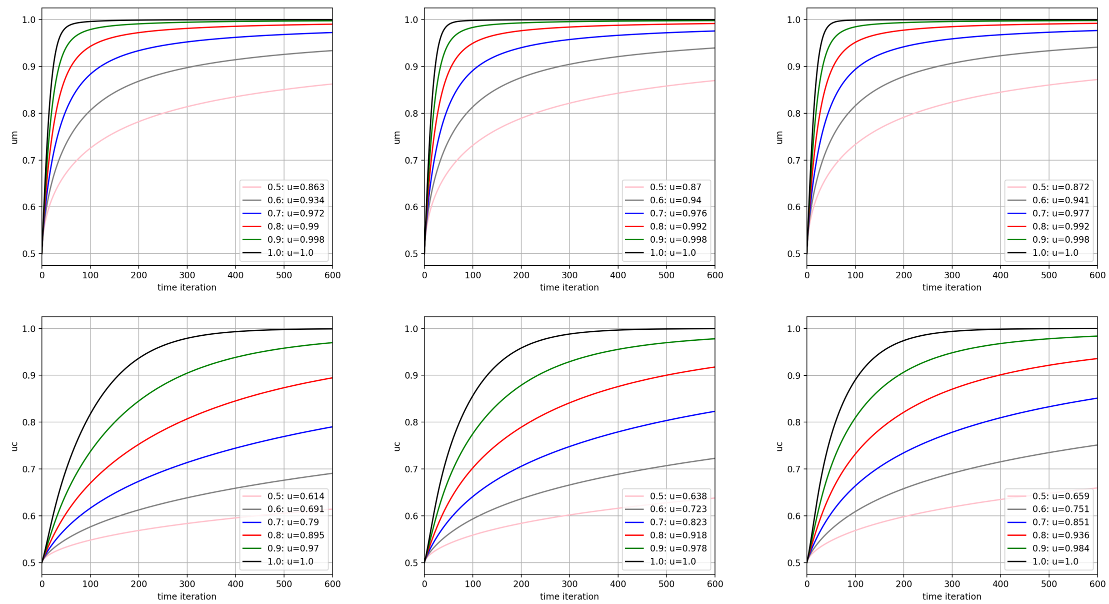

Figure 5.34: Heterogeneity 1. Geometry 1, 2 and 3 (from left to right)

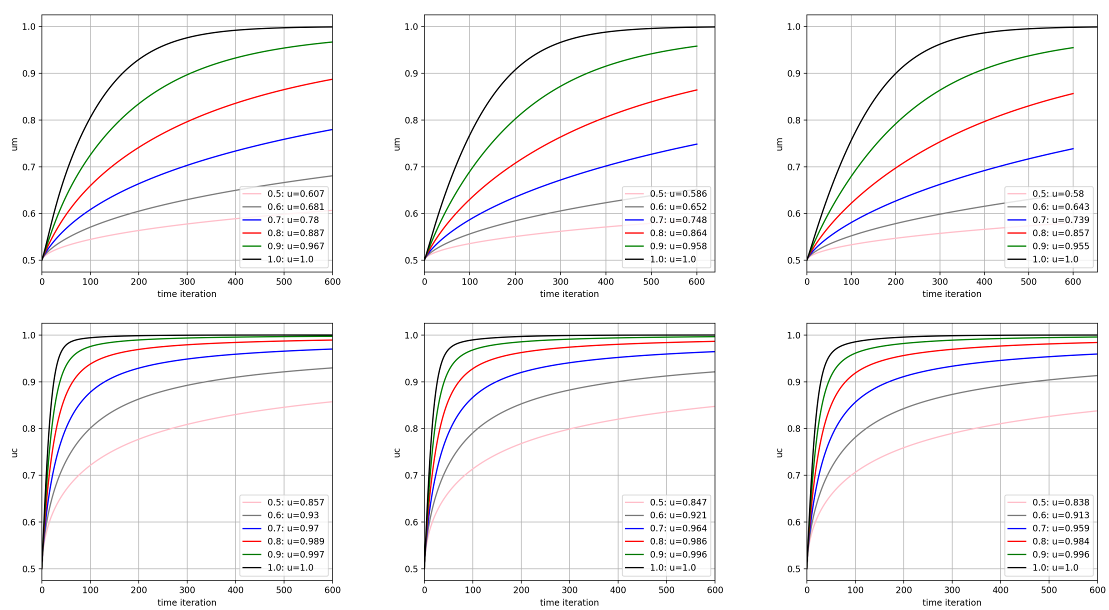

Figure 5.35: Heterogeneity 2. Geometry 1, 2 and 3 (from left to right)

CHAPTER 6: CONCLUSIONS

The spatial-temporal models of one and two-species population distribution are considered in heterogeneous domains with circle inclusions. An unsteady diffusion-reaction equation describes mathematical models with a nonlinear reaction term. The unstructured grid resolves inclusions on the grid level for accurate space approximation. A discrete system is constructed based on the semi-implicit time approximation scheme and finite element method. Numerical results were presented for the one-species and two-species interaction models for three geometries with different volumes of the inclusions to illustrate the influence of the geometry on time to reach equilibrium and the solution dynamic. The parameters' influence is investigated for different values of the diffusion, expansion rate, interaction term, and initial condition. The results illustrate a huge influence of heterogeneity on the dynamic of the solution and the time to reach equilibrium.

In this study, we investigated initial-boundary value issues for models of one and two species of populations. We started our investigation by using these models with the semi-implicit time approximation method. By using the solutions from the previous time layer, we were able to linearize the complex response dynamics and make the problem more manageable. This approach gave us equations that precisely capture the behaviour of the models, opening the door for more detailed analysis.

Our set of equations was then transformed into a variational representation of the problem, which elegantly integrated the key variables. We were able to reframe our modelas one of finding a function within a specified function space that satisfied the required equations as a result of this transformation. Thus, the bilinear and linear forms for both models were defined, greatly strengthening the mathematical elegance of our approach.

Then, in an effort to use our growing mathematical understanding in a more practical context, we turned to a discrete system. To define discrete spaces on this grid, we triangulated the domain in this section. This method improved the problem's computing viability by encapsulating the problem's continuous character within a discrete framework. Additionally, we switched from variational formulations to their corresponding matrix forms, which allowed us to methodically resolve these complicated models.

We have studied the time-fractional diffusion-reaction equations for the dynamics of population expansion in diverse environments. Our research has thrown important light on the behaviour of populations in various ecological systems and shown the complex interactions between diffusion, response, and domain heterogeneity. We have developed a more precise and sophisticated modelling framework that incorporates fractional derivatives to capture memory effects and long-term dependencies, which are essential to grasping ecological processes.

We investigated the sensitivity of population dynamics to important variables including diffusion coefficients and expansion rates through numerical simulations. The necessity of taking into account both diffusion and reaction mechanisms in ecological modelling is shown by the fact that different combinations of these elements result in different patterns of population increase or decline.

The study that was conducted offers a thorough method for comprehending the intricate phenomena of population dynamics in single- and dual-species systems. The approaches and techniques used have a strong theoretical foundation and are computationally feasible, from semi-implicit temporal approximations through variational formulations and further into discrete systems. As we continue to create more sophisticated and effective methods for revealing the complex dynamics of biological populations, this study leaves us well-prepared for additional research in this area.

REFERENCES

James Ahrens, Berk Geveci, and Charles Law. Paraview: An end-user tool for large data visualization. *The visualization handbook*, 717(8), 2005.

Grégoire Allaire, Robert Brizzi, Andro Mikelić, and Andrey Piatnitski. Two-scale expansion with drift approach to the taylor dispersion for reactive transport through porous media. *Chemical Engineering Science*, 65(7):2292–2300, 2010.

Ilenia Battiato, Daniel M Tartakovsky, Alexandre M Tartakovsky, and Timothy D Scheibe. Hybrid models of reactive transport in porous and fractured media. *Advances in Water Resources*, 34(9):1140–1150, 2011.

Gaurav Bhatnagar, Walter G Chapman, Gerald R Dickens, Brandon Dugan, and George J Hirasaki. Generalization of gas hydrate distribution and saturation in marine sediments by scaling of thermodynamic and transport processes. *American Journal of Science*, 307(6):861–900, 2007.

Zachary P Chairez. *Spatial-Temporal Models of Multi-Species Interaction to Study Impacts of Catastrophic Events*. PhD thesis, Texas A&M University-Corpus Christi, 2020.

Eric T Chung, Uygulaana Kalachikova, Maria Vasilyeva, and Valentin Alekseev. Generalized multiscale discontinuous galerkin method for convection–diffusion equation in perforated media. *Mathematics and Computers in Simulation*, 193:666–688, 2022.

Christophe Geuzaine and Jean-François Remacle. Gmsh: A 3-d finite element mesh generator with built-in pre-and post-processing facilities. *International journal for numerical methods in engineering*, 79(11):1309–1331, 2009.

Alexandr Kolesov, Petr Vabishchevich, and Maria Vasilyeva. Splitting schemes for poroelasticity and thermoelasticity problems. *Computers & Mathematics with Applications*, 67(12):2185–2198, 2014.

Svyatoslav Korneev and Ilenia Battiato. Sequential homogenization of reactive transport in polydisperse porous media. *Multiscale Modeling & Simulation*, 14(4):1301–1318, 2016.

Anders Logg, Kent-Andre Mardal, and Garth Wells. *Automated solution of differential equations by the finite element method: The FEniCS book*, volume 84. Springer Science & Business Media, 2012.

Gurii Ivanovich Marchuk. *Mathematical models in environmental problems*. Elsevier, 1986.

Paul A. Montagna, Alexey L. Sadovski, Scott A. King, Kevin K. Nelson, Terence A. Palmer, and Kenneth H. Dunton. Modeling the effect of water level on the Nueces Delta marsh community. *Wetlands Ecology and Management*, 25(6):731–742, December 2017.

James Dickson Murray. *Mathematical biology: I. An introduction*. Springer, 2002.

Akira Okubo and Simon A Levin. *Diffusion and Ecological Problems: Modern Perspectives*, volume 14. Springer, 2001.

AD Polyanin. Exact solutions of nonlinear sets of equations of the theory of heat and mass transfer in reactive media and mathematical biology. *Theoretical Foundations of Chemical Engineering*, 38(6):622–635, 2004.

Denis Spiridonov, Maria Vasilyeva, and Wing Tat Leung. A generalized multiscale finite element method (gmsfem) for perforated domain flows with robin boundary conditions. *Journal of Computational and Applied Mathematics*, 357:319–328, 2019.

Petr Vabishchevich and Maria Vasilyeva. Explicit-implicit schemes for convection-diffusion-reaction problems. *Numerical Analysis and Applications*, 5(4):297–306, 2012.

Petr N Vabishchevich. Additive operator-difference schemes. In *Additive Operator-Difference Schemes*. de Gruyter, 2013.

Maria Vasilyeva. Efficient decoupling schemes for multiscale multicontinuum problems in fractured porous media. 2022.

Maria Vasilyeva, Eric T Chung, Wing Tat Leung, Yating Wang, and Denis Spiridonov. Upscaling method for problems in perforated domains with non-homogeneous boundary conditions on perforations using non-local multi-continuum method (nlmc). *Journal of Computational and Applied Mathematics*, 357:215–227, 2019.

Maria Vasilyeva, Alexey Sadovski, and D. Palaniappan. Multiscale solver for multi-component reaction-diffusion systems in heterogeneous media. 2022.

Maria Vasilyeva, Youwen Wang, Sergei Stepanov, and Alexey Sadovski. Numerical investigation and factor analysis of the spatial-temporal multi-species competition problem. 2022.